Phycologia Volume 53 (3), 265–292 Published 22 May 2014

On *Levanderina fissa gen. & comb. nov.* (Dinophyceae) (syn. *Gymnodinium fissum*, *Gyrodinium instriatum*, *Gyr. uncatenum*), a dinoflagellate with a very unusual sulcus

Øjvind Moestrup[1]*, Päivi Hakanen[2], Gert Hansen[1], Niels Daugbjerg[1], and Marianne Ellegaard[3]

[1]*Marine Biological Section, Department of Biology, University of Copenhagen, Universitetsparken 4, DK-2100 Copenhagen Ø, Denmark*
[2]*Marine Research Centre, Finnish Environment Institute, P.O. Box 140, FI-00251 Helsinki, Finland*
[3]*Department of Plant and Environmental Sciences (PLEN), University of Copenhagen, Thorvaldsensvej 40, DK-1871 Frederiksberg C, Denmark*

Abstract: *Gymnodinium fissum* was described by Levander in 1894 from the Baltic Sea near Helsinki, and we argue, on the basis of morphological and molecular studies of material from the type locality, and on cultures from the Åland islands, Puerto Rico, Portugal and United States identified as *Gyrodinium instriatum*, *Gymnodinium instriatum*, *Gyrodinium uncatenum* and *Gyrodinium* sp., that all these taxa are conspecific. They are morphologically and genetically distinct from *Gymnodinium* and are described here as *Levanderina fissa gen. & comb. nov*. This species also includes *Gyrodinium pavillardii*. Levander observed chloroplasts in the cell and on some occasions diatoms, probably the first report of mixotrophy in a dinoflagellate. Biecheler in 1952 described the process of food uptake in *Gyr. pavillardii*, feeding it with ciliates and other dinoflagellates. Prey was taken up through the posterior part of the sulcus, some prey items being almost as large as the host. Our observations showed that the longitudinal flagellum, in contrast to what has been described in all other dinoflagellates possessing a longitudinal sulcal furrow, is not located in the furrow but in a separate, internal tube beneath the sulcal furrow. The tube opened to the exterior dorsally near the posterior end of the cell, and the sulcus appeared to be used for food uptake only. The cytoskeleton of *L. fissa* was complex and included a large number of muscle-like fibres. Food uptake using the sulcus involved major changes of cell shape, which requires the presence of a highly flexible cytoskeleton. *Levanderina fissa* was not morphologically or genetically close to any other dinoflagellate for which molecular sequences were available. The detailed structure of the apical furrow or acrobase comprised three rows of elongate vesicles, one row forming the bottom of a furrow. The new term apical structure complex (ASC) is introduced as a general term to replace apical furrow or acrobase, none of which adequately describes all the many known types. The ASC in *Levanderina* may be characteristic of most if not all species of the Gymnodiniales (an apomorphy of the order?) and different from the types present in the Suessiales, the other order of mainly thin-walled dinoflagellates.

Key Words: Dinoflagellates, Mixotrophy, Phylogeny, Ultrastructure

INTRODUCTION

In 1894 Levander described a new unarmoured dinoflagellate from coastal waters near the island of Lövö in southern Finland, naming it *Gymnodinium fissum* Levander (Levander 1894). Shortly afterward it was transferred by Lemmermann (1900) to the genus *Spirodinium* [*S. fissum* (Levander) Lemmermann], and subsequently Kofoid & Swezy (1921) moved it to their new genus *Gyrodinium* [*G. fissum* (Levander) Kofoid & Swezy]. The latter change was due to the cingular displacement exceeding 1/5 of the body length, the generic definition of *Gyrodinium*. Levander's description was quite detailed with respect to cell shape, cingulum, sulcus and internal structures. He mentioned, but did not illustrate, delicate surface striations that were present on a few cells. It was therefore not in accordance with his description when Kofoid & Swezy (1921) depicted cells with distinct striae from offshore La Jolla, California, USA, which they claimed to belong to Levander's species. Kofoid & Swezy were even able to count the striae: '24 across the ventral surface of the epicone, and twice as many on the hypocone'. When Biecheler found material from Étang de Thau, France, which was very similar to Levander's material, the lack of striation and presence of metabolic activity probably led her to describe it as a new species, *Gyrodinium pavillardii* ['pavillardi'] Biecheler (Biecheler 1952), although these features were not mentioned in her first, more incomplete report of the species (Biecheler 1934). The lack of striations finally led Freudenthal & Lee (1963), who seemed to be unaware of Biecheler's descriptions of *Gyr. pavillardii,* to establish the new species *Gyr. instriatum* Freudenthal & Lee on the basis of material from Long Island, New York, USA. They stressed its strong resemblance to Levander's *Gyr. fissum* and to *Gyr. uncatenum* Hulburt, a species described a few years before from Uncatena Island near Woods Hole, Massachusetts, USA (Hulburt 1957).

Gyrodinum instriatum has subsequently been found in fully saline and brackish waters from many areas of the world. It was transferred to *Gymnodinium* as *Gymnodinium instriatum* (Freudenthal & Lee) Coats because of the similarity between its apical furrow and that of *Gymnodinium* (Coats & Park 2002). Hällfors (2004) regarded *Gyr. instriatum* and *Gyr. pavillardii* as junior synonyms of *Gyr. fissum*, and did not agree that *Gyr. fissum sensu* Kofoid & Swezy (1921) represented Levander's species. His conclusion was very

* Corresponding author (moestrup@bio.ku.dk).
DOI: 10.2216/13-254.1

Table 1. List of dinoflagellate cultures examined in the present study. The strains with CCMP codes in parentheses were originally deposited in the NCMA culture collection, but were used for this study from the SCCAP collection.

Species (as indicated in culture collection)	Origin	Culture code	Isolated by	GenBank accession number
Gymnodinium fissum	Stora Lövö, Espoo, Finland*	K-1769 (GFL1103)	Hakanen, P.	
Gymnodinium fissum	Åland, Finland	K-1727 (GFF1001)	Hakanen, P.	
Gymnodinium fissum	Åland, Finland	K-1768 (GFF1101)	Hakanen, P.	
Gyrodinium instriatum	Rhode River, USA	K-0641	Cooney, S.	
Gyrodinium instriatum	Santo Andre lagoon, Portugal	K-0675 (CCMP431)	Silva, E.	EF205007
Gyrodinium instriatum	Texas, Gulf of Mexico, USA	K-1067 (CCMP1737)		EF205008
Gyrodinium sp.	Mosquito Bay, Puerto Rico	K-1273 (CCMP3173)	Russell, J.	
Gyrodinium uncatenum	Perch Pond, Falmouth, Massachusetts, USA	CCMP1310	Kulis, D.	

* Strain from the type locality of *Gymnodinium fissum*.

plausible but has not been generally accepted. Our purpose was therefore, by combining molecular and ultrastructural analyses, to investigate the possible synonymy of *Gyr. fissum* and *Gyr. instriatum*, on the basis of material collected from several localities in the Baltic Sea, including the type locality of *Gyr. fissum* and material of *Gyr. instriatum* from several different geographical localities.

Furthermore, with the advent of the molecular era, numerous studies on dinoflagellate phylogeny have consistently shown that *Gyrodinium instriatum* and *Gyr. uncatenum* form a well-supported clade, distinct from *Gyr. spirale*, the type species of *Gyrodinium*, and from all other unarmoured dinoflagellates studied so far (*e.g.* Saldarriaga *et al.* 2004; Kim & Kim 2007), suggesting that it belongs in a genus of its own. In the present study, material considered to represent Levander's species is compared with the taxonomic criteria introduced to define unarmored dinoflagellates by Daugbjerg *et al.* (2000). The system proposed by these authors, and supported by molecular data, was based primarily on ultrastructural details such as the structure of the apical groove, the nuclear envelope, and details of the flagellar apparatus. The findings reported during the present study have led us to propose a new genus, *Levanderina gen. nov.* with a single known species, *Levanderina fissa comb. nov.*

MATERIAL AND METHODS

Cultures used during the present study were retrieved from culture collections or established from water or sediment samples collected in the Baltic region. The cultures were established by single-cell or cyst isolations during the period July 2010–July 2011; the cultures included several strains from the Åland Archipelago as well as strain K-1769 from Lövö, the type locality of *Gymnodinium fissum*. The cultures were grown at 16°C in f/2 medium (salinity = 6). Two strains from Åland and one from Lövö were deposited in the Scandinavian Culture Collection for Algae and Protozoa (SCCAP) at the University of Copenhagen (Table 1). Other cultures were obtained from SCCAP (K strain codes) and Provasoli-Guillard National Center for Marine Algae and Microbiota (NCMA) (CCMP strain code). Growth conditions for the different K strains are available at the home page of SCCAP (http://www.sccap.dk) and for the CCMP strains at the home page of NCMA (https://ncma.bigelow.org/). Strain CCMP1310 originates less than 20 km from the type locality of *Gyrodinium uncatenum* and strain K-0641 around 300 km from the type locality of *Gyr. instriatum*. Table 1 summarizes information on strain numbers and origin of cultures for which molecular sequences were determined during the present study.

Live cultures were examined using Olympus (BX51/Provis AX70; Olympus Corp., Tokyo, Japan) or Zeiss Axioplan (Carl Zeiss, Göttingen, Germany) light microscopes equipped with differential interference contrast optics. Photodocumentation was performed using Zeiss Axio Cam HR or Olympus DP72 digital cameras, or a SVCam 085 digital video camera (SVS-Vistek Cameras, Seefeld, Germany). Images from video sequences were grabbed using Video Savant Pro (IO Industries Inc., Ontario, Canada). Chloroplast autofluorescence was studied in live cells using an inverted Olympus IX81 microscope equipped with a disk-spinning unit. Micrographs were taken with a black and white digital camera FViewII (Olympus Soft Imaging System, Tokyo, Japan).

For scanning electron microscopy (SEM) of the vegetative stage, cells were fixed for 20 min in a final concentration of 2% OsO_4 and 0.1% glutaraldehyde in distilled water. Strains K-0675 and K-1067 were fixed only in 2% OsO_4 in 0.2-μm-filtered seawater. After fixation, cells were filtered onto an Isopore membrane filter (8 μm pore size) (Millipore) and washed with distilled water for 30 min. They were dehydrated in an ethanol series: 10 min in each concentration of 30%, 50%, 70%, 90%, 96% and 99.9%, followed by two steps of 30 min each in absolute ethanol at 4°C. Cells were critical-point-dried in a Bal-Tec CPD 030 (Bal-Tec AG, Balzers, Liechtenstein) and sputter coated with platinum–palladium or gold in a JEOL JFC-2300HR sputter (JEOL Ltd., Tokyo, Japan) before examination in a JEOL JSM-6333F field-emission scanning electron microscope operated at 7 kV. For SEM of the resting stage, *c.* 40 cysts of the K-1727 culture were isolated and fixed in acid Lugol's solution for 30 min. They were subsequently treated and examined as described above.

For transmission electron microscopy (TEM), strain K-1727 was fixed using two different schedules. Schedule 1: equal volumes were mixed of culture and 4% glutaraldehyde made up in 0.2 M Na-cacodylate buffer and containing 0.1 M sucrose at pH 7.8, and the cells were fixed for 2 h at 4°C. They were pelleted by centrifugation, and washed with 0.2 M

Table. 2. Sequence divergence in percentage of sequence pairs between groups with identical LSU rDNA or single species as indicated in the table. In total 963 base pairs were included in the estimation, which used the Kimura 2-parameter model; a and b indicate identical sequences, respectively.

Species/strains	*G. fuscum*	K-641	EF613345/ GUSW00/ GUDE00	K-1727/ K-1067/ K-1769	K-675	K-1768	K-1273	CCMP 1310
G. fuscum	–							
K-0641	23.9	–						
EF613345a	23.9	0.23	–					
GUSW00a								
GUDE00a								
K-1727b	25.0	0.91	0.91	–				
K-1067b								
K-1769b								
K-0675	32.6	1.02	1.02	0.13	–			
K-1768	25.2	1.37	1.37	0.45	0.57	–		
K-1273	24.2	0.34	0.57	1.25	1.37	1.71	–	
CCMP 1310	24.2	0.23	0.45	1.14	1.25	1.60	0.34	–

Na-cacodylate buffer containing 0.1 M sucrose for 30 min at 4°C, followed by buffer without sucrose for 30 min at 4°C. Postfixation was in 1% OsO_4 made up in distilled water for 1 h at 4°C. After rinsing in 0.2 M Na-cacodylate buffer, cells were dehydrated in a graded ethanol series. They were embedded in Spurr's resin after two 5-min steps in propylene oxide. Sections (50–-60 nm) were cut with a diamond knife using a Leica Super Nova microtome (Leica Microsystems GmbH, Wetzlar, Germany) and placed on copper grids. They were stained in uranyl acetate and lead citrate and examined in a JEOL JEM-1010 electron microscope operated at 80 kV (JEOL Ltd, Tokyo, Japan). All micrographs were taken on a Gatan Orius digital camera (Gatan Inc., Pleasanton, California, USA). Schedule 2: cells were fixed for 30 min at 4°C by mixing one volume of culture with one volume of fixative containing 4% glutaraldehyde and 1% OsO_4 in 0.2 M Na-cacodylate buffer, the latter containing 0.1 M sucrose at pH 7.4. Cells were pelleted by centrifugation and washed twice in 0.2 M Na-cacodylate buffer for 5 min. These steps were followed by postfixation in 1% OsO_4 in 0.2 M Na-cacodylate buffer for 1 h at 4°C. Subsequent steps followed schedule 1.

For DNA extraction, exponentially growing cultures (approximately 10–15 ml) were harvested by centrifugation at 2500 revolutions per minute (rpm) (=1201 g) for 10–15 min. The resulting cell pellets were transferred to Eppendorf tubes and frozen at –18°C, preserved in 96% ethanol or used directly for DNA extraction. For strain CCMP 1310, total genomic DNA was extracted as outlined in Daugbjerg *et al.* (1994). For strains K-1727, K-1768, K-0641 and K-1273, cells were broken with a motor pestle and DNA was extracted using a DNeasy Plant Mini Kit (Qiagen, Chatsworth, California, USA) according to the manufacturer's instructions. For strain K-1769, single cells were isolated into a drop of sterile distilled water, frozen at –20°C and used for single-cell polymerase chain reaction (PCR).

Extracted DNA served as a template to PCR to amplify partial, nuclear-encoded large-subunit ribosomal DNA (LSU rDNA). Two primer combinations (D1R-D3B and D1R-28-1483R) were used for sequence determination of approximately 950 and 1450 base pairs, respectively. For strains K-1727, K-1768, K-1769, K-0641 and K-1273, amplification was in 25 µl of a solution containing 2.5 units of PuReTaq DNA polymerase, 10 mM Tris-HCl, pH 9.0, 50 mM KCl, 1.5 mM $MgCl_2$, 200 µM of each of deoxynucleotide triphosphate, stabilizers, and bovine serum albumin (BSA) (illustra PuReTaq Ready-To-Go^{TM} PCR beads, GE Healthcare Bio-Sciences Corp., Piscataway, New Jersey, USA), 1 µl of extracted sample and 1 µl of each 10 µM primer. PCR conditions comprised an initial denaturation at 95°C for 5 min, 30 cycles of denaturation at 95°C for 2 min, annealing at 54°C for 4 min, extension at 72°C for 2 min, and a final extension at 72°C for 7 min. DNA fragments were checked in a 2% agarose gel containing ethidium bromide and visualized with ultraviolet light. Successful PCR products were sent for sequencing to the Institute of Biotechnology (University of Helsinki, Finland). PCR products were purified here by MultiScreen PCR_{96} (Merck-Millipore Corp., Billerica, Massachusetts, USA) before sequencing using a BigDye® Terminator v3.1 Cycle Sequencing Kit (Applied Biosystems, Life Technologies Corporation, Carlsbad, California, USA), following the protocol recommended by the manufacturer. The sequencing reactions were cleaned using an Agencourt® CleanSEQ kit (Beckman Coulter Inc., Brea, California, USA) and run with an ABI 3130XL Genetic Analyzer (16 capillaries) or an ABI 3730 DNA Analyzer (48 capillaries) (Applied Biosystems). Primers used in sequencing were D1R, D2R and D2C (Scholin *et al.* 1994), D3A and D3B (Nunn *et al.* 1996).

For strain CCMP 1310, amplification conditions and temperature profiles were as described in Hansen and Daugbjerg (2011). PCR products were purified following the instructions of the QIAquick PCR purification Kit (Qiagen). Nucleotide sequences were determined using the Dye Terminator Cycle Sequencing Ready Reaction Kit (Perkin Elmer, Foster City, California, USA), according to the recommendation of the manufacturer. The cycle sequencing reactions were run on an ABI PRISM 377 DNA Sequencer (Perkin Elmer).

We aimed at determining the LSU rDNA sequence from a number of dinoflagellates that morphologically resembled *Gyrodinium uncatenum*, *Gyr. instriatum* and *Gymnodinium fissum*, and we included sequences of eight strains, in addition to the strains from Finland. The sequences and

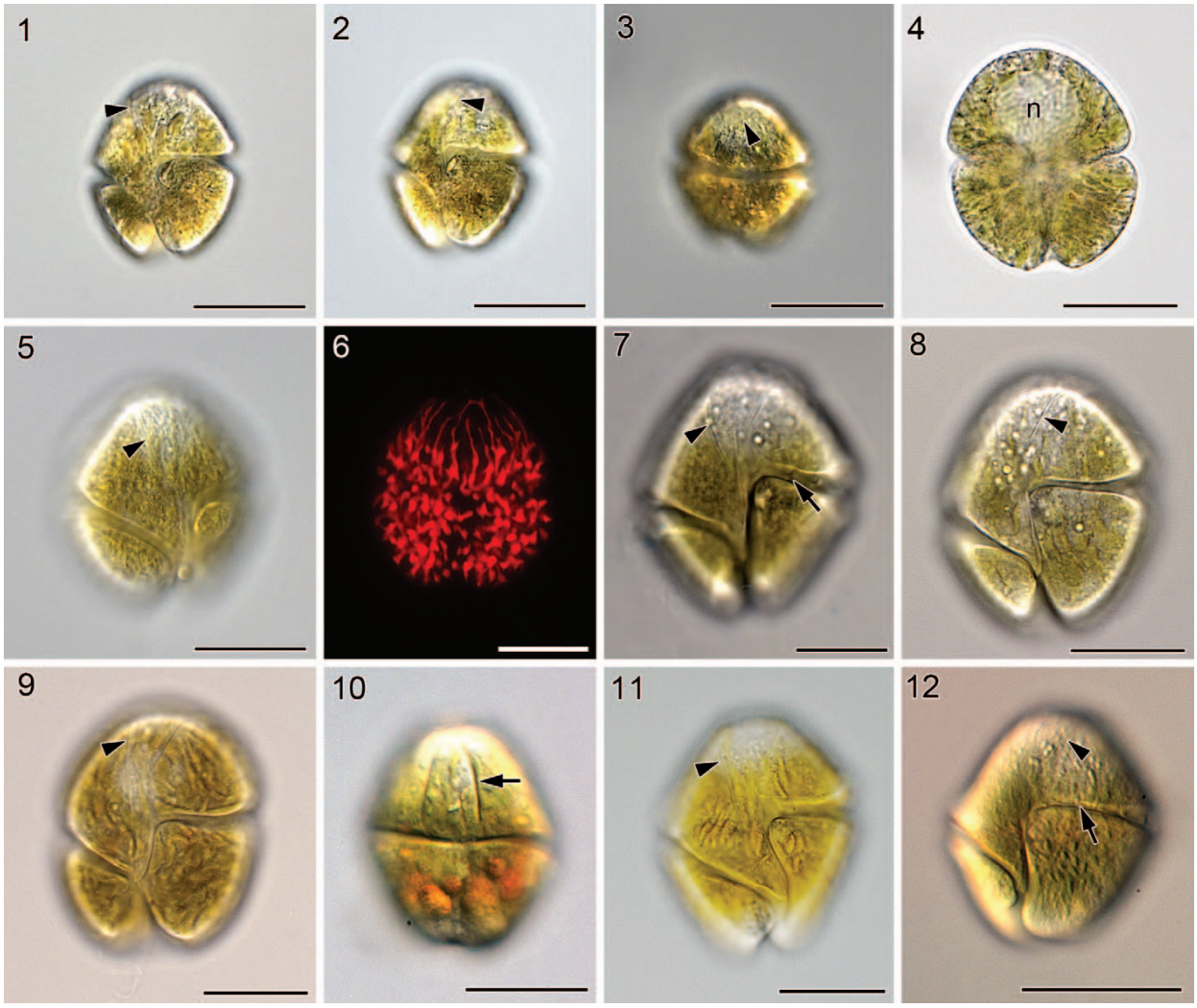

Figs 1–12. Light microscopy of living cells of *Levanderina fissa comb. nov*. Scale bars = 20 μm.
Figs 1–4. Strain K-1769 from the type locality of *Gymnodinium fissum* at Lövö, southern Finland.
Figs 1, 2. Ventral view of the same cell at different focal levels showing the ASC (arrowhead).
Fig. 3. ASC (arrowhead) from the dorsal side.
Fig. 4. Deeper focal level showing spherical nucleus (n) in the epicone.
Figs 5, 6. Strain K-1727 from the Åland Islands, Finland.
Fig. 5. Ventral view, ASC (arrowhead).
Fig. 6. Epifluorescence micrograph showing chloroplasts.
Fig. 7. Strain K-0641 from the Rhode River, USA. Ventral view, ASC (arrowhead), transverse flagellum (arrow).
Fig. 8. Strain K-0675 from the Santo Andre lagoon, Portugal. Ventral view, ASC (arrowhead).
Figs 9, 10. Strain K-1067 from Texas, Gulf of Mexico.
Fig. 9. Ventral view, ASC (arrowhead).
Fig. 10. Dorsal view, furrows (arrow) in the epicone.
Fig. 11. Strain K-1273 from Puerto Rico. Ventral view, ASC (arrowhead).
Fig. 12. Strain CCMP 1310 from Perch Pond, Falmouth, Massachusetts, USA. Ventral view, ASC (arrowhead), transverse flagellum (arrow).

the LSU rDNA sequence from a single isolate of *Gyr. instriatum* and two isolates of *Gyr. uncatenum* available in GenBank were added to a data matrix recently compiled to describe the dinoflagellate genus *Moestrupia* (Hansen & Daugbjerg 2011). This alignment comprised 71 taxa, and due to ambiguous alignment of the highly divergent domain D2 (*sensu* Lenaers *et al*. 1989) this domain was omitted, leaving 746 base pairs. Of the 71 taxa, 62 were dinoflagellates, the rest being ciliates (three taxa), apicomplexans (five taxa) and the perkinsid *Perkinsus*. The latter groups comprised the outgroup. The sequence data matrix was edited using SeaView (ver. 4.3.2) by Gouy *et al*. (2010). For phylogenetic

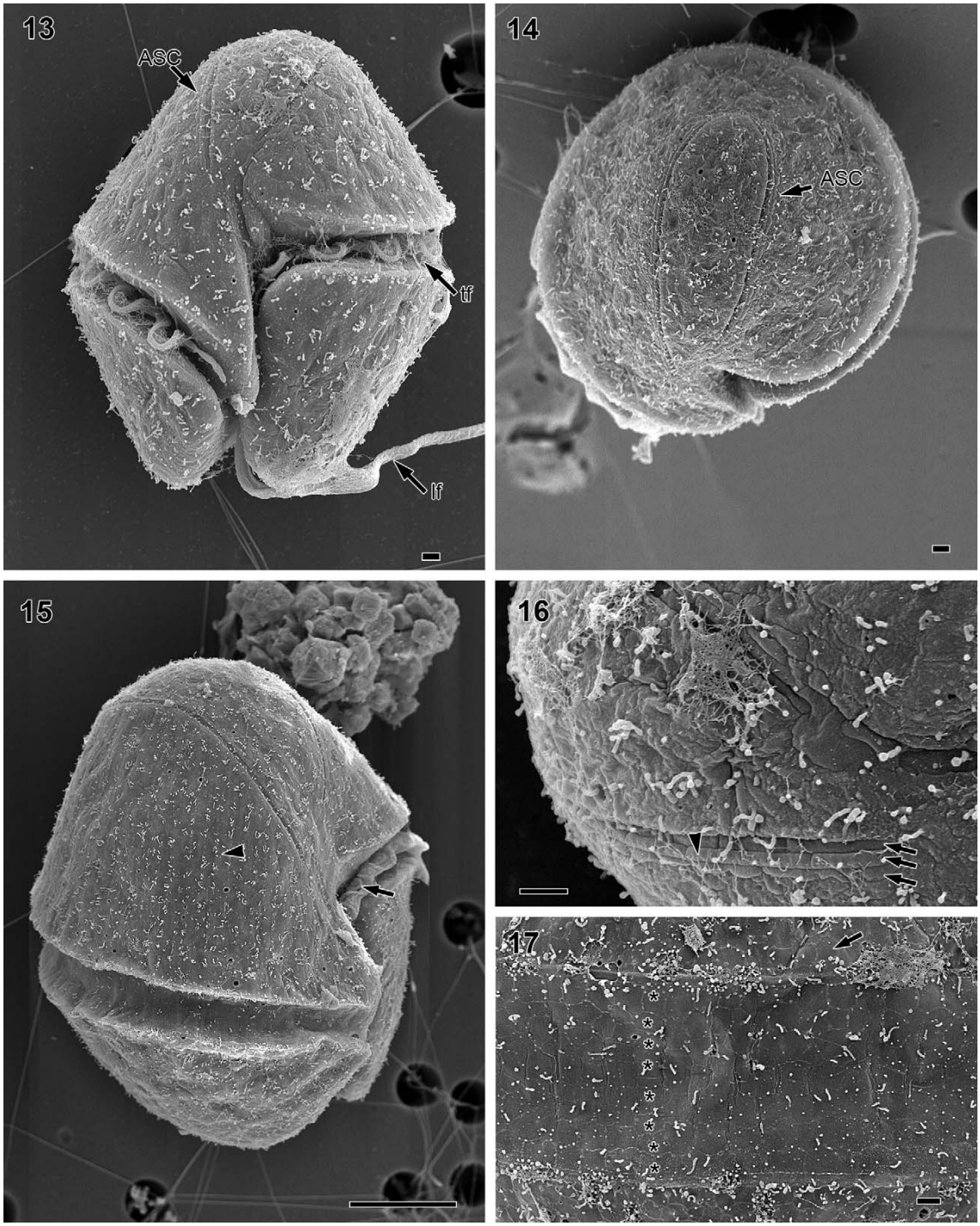

Figs 13–17. SEM of *Levanderina fissa comb. nov.* (K-1769) from the type locality of *Gymnodinium fissum* at Lövö, Finland.
Fig. 13. Ventral view, ASC, transverse (tf) and longitudinal flagellum (lf). The longitudinal furrow appears empty as it does not contain the longitudinal flagellum. This flagellum runs in an internal tube that opens in the posterior part of the cell; compare with Fig. 23. Scale bar = 1 μm.
Fig. 14. Apical view, showing the long U-shaped ASC. Scale bar = 1 μm.
Fig. 15. Planozygote in right lateral view. Notice the duplicated transverse flagellum (arrows) and faint striations (arrowhead). Scale bar = 10 μm.
Fig. 16. ASC consists of three rows of rectangular amphiesmal vesicles (arrows), the topmost row located at a slightly deeper level in the cell. Fine fibrils extrude from the central row (arrowhead). Scale bar = 1 μm.
Fig. 17. Cingulum comprises eight horizontal rows of amphiesmal vesicles (asterisks). Arrow indicates the amphiesmal vesicle on the epicone. Scale bar = 1 μm.

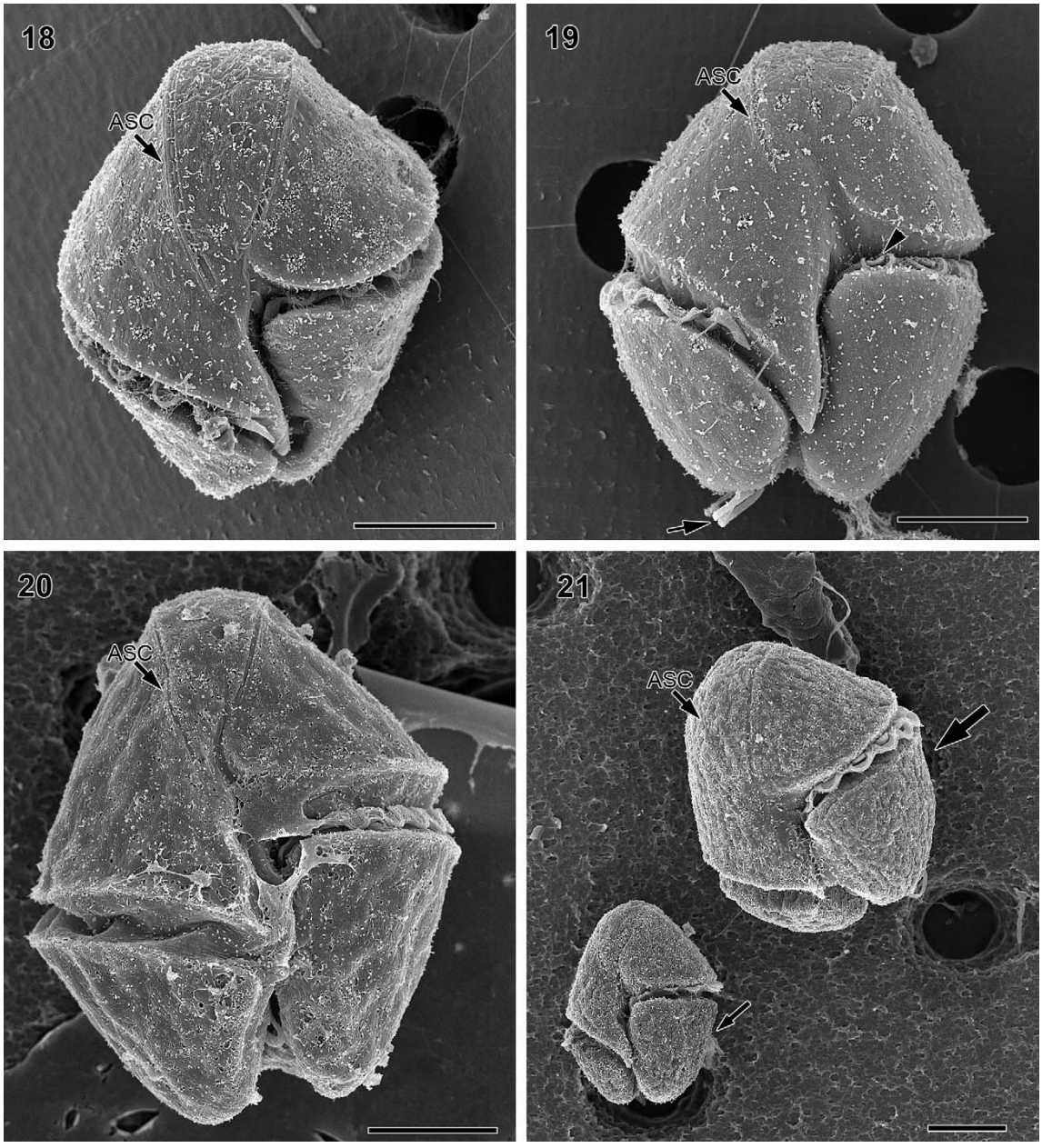

Figs 18–21. SEM of *Levanderina fissa comb. nov*. Scale bars = 10 μm.
Fig. 18. Strain K-1768 (*Gymnodinium fissum*) from Åland, Finland, in ventral view.
Fig. 19. Strain K-0641 (*Gyrodinium instriatum*) from the Rhode River, USA, planozygote in ventral view. Both the longitudinal and the transverse flagella have duplicated (arrowhead and arrow, respectively).
Fig. 20. Strain K-1067 (*Gyrodinium instriatum*) from Gulf of Mexico, Texas, in ventral view.
Fig. 21. Strain K-0675 (*G. instriatum)* from Portugal, vegetative cell (small arrow) and planozygote (large arrow), both in ventral view. ASC, apical structure complex in all figures.

inference we used two approaches: Bayesian analysis (BA) as implemented in MrBayes (ver. 3.1.2 by Ronquist & Huelsenbeck 2003) and maximum likelihood (ML) analysis as implemented in PhyML (ver. 3.0 by Guindon & Gascuel 2003). BA used a general time-reversible substitution model with base frequencies and substitution rate matrix estimated from the data. It was run for two million Markov chain Monte Carlo generations with four parallel chains. For every 50th generation a tree was sampled, and the burn-in was evaluated by plotting the LnL values as a function of generations using Microsoft Excel. The graph revealed a burn-in after 20,050 generations, leaving 39,600 trees for

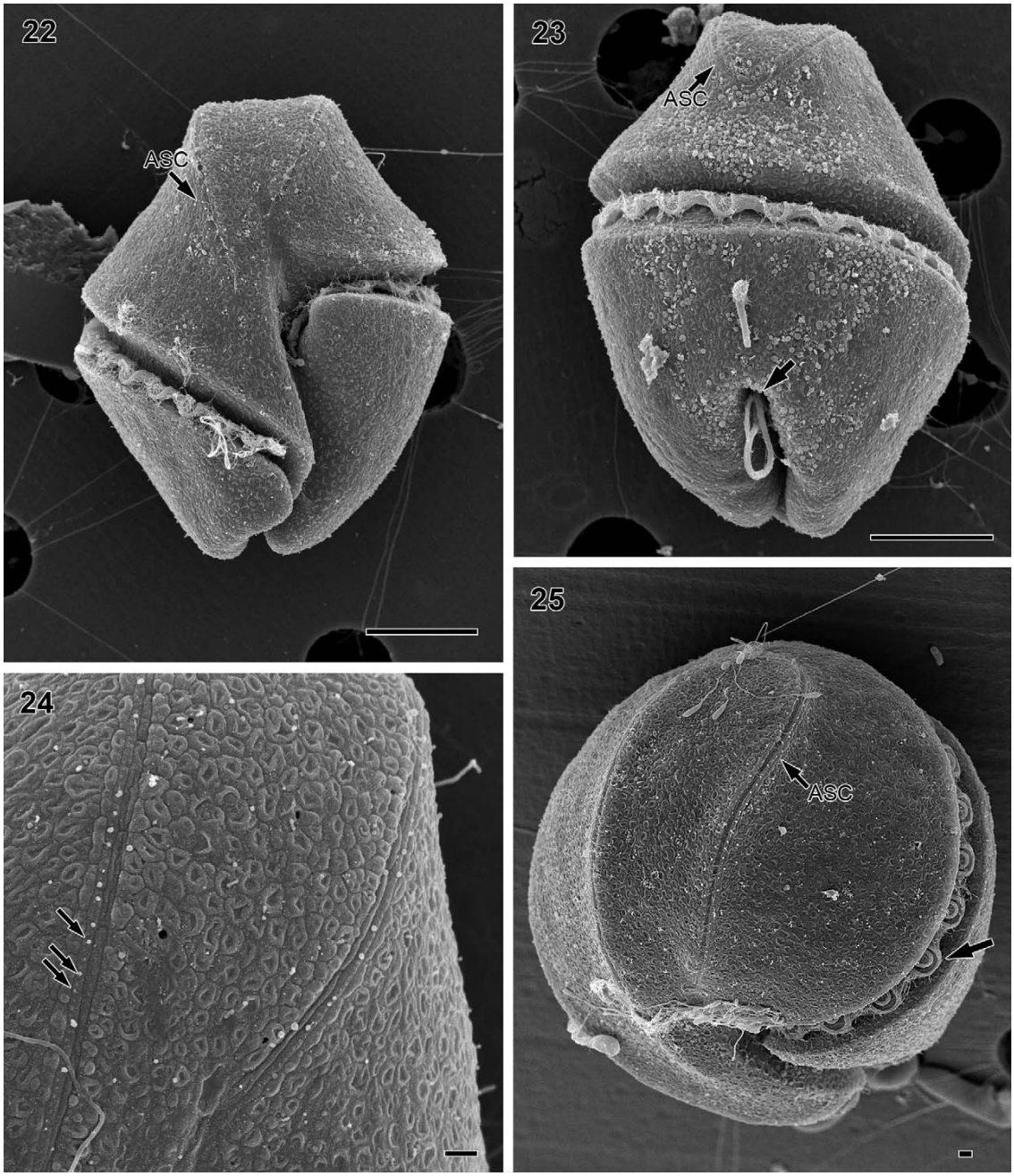

Figs 22–25. SEM of *Levanderina fissa comb. nov.*, all showing strain K-1273 from Puerto Rico.
Fig. 22. Ventral view. Scale bar = 10 μm.
Fig. 23. Dorsal view showing the deeply incised and the dorsal emergence of the longitudinal flagellum from the sulcus (arrow). Scale bar = 10 μm.
Fig. 24. Details of the ASC. The amphiesmal vesicles of the central row possess small knobs (arrows). Scale bar = 1 μm.
Fig. 25. Planozygote in apical view. The transverse flagellum has duplicated (arrow). Scale bar = 1 μm.

estimating posterior probabilities. Hence, 401 trees were discarded. Posterior probability values were obtained from a 50% majority-rule consensus of the 39,600 saved trees using PAUP* (ver. 4b10 of Swofford 2003). Before running the ML analysis, we used Modeltest (ver. 3.7 by Posada & Crandall 1998) to choose the best among 56 predefined models for our data set (results not shown). To understand the robustness of the ML tree topology we used bootstrapping with 100 replications. BA was run on a desktop computer, whereas we used the South of France bioinfor-

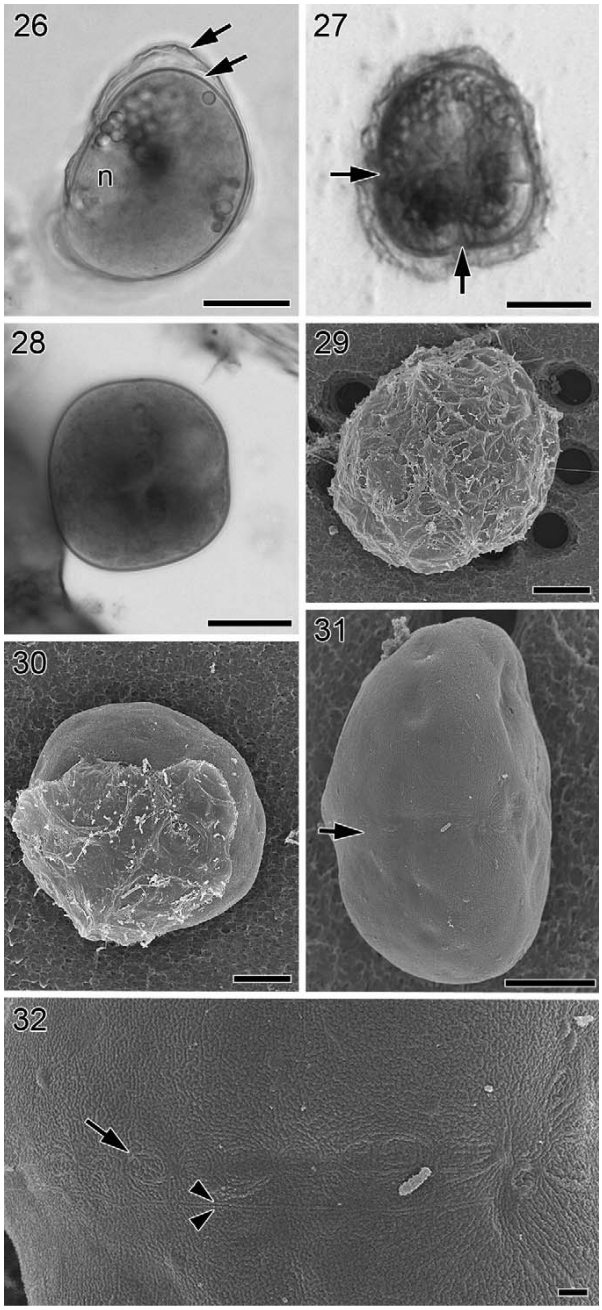

Figs 26–32. Cysts of *Levanderina fissa comb. nov.* light microscopy and SEM.

Fig. 26. Inner and outer layers are marked by arrows. The nucleus (n) is visible. Scale bar = 20 μm.

Fig. 27. Cyst showing indications of paracingulum and parasulcus (arrows). Scale bar = 20 μm.

Fig. 28. Cyst without the second layer. Scale bar = 20 μm.

Fig. 29. SEM of the outer membranous layer. Scale bar = 10 μm.

Fig. 30. SEM of a cyst partially covered with the outer layer. Scale bar = 10 μm.

Fig. 31. SEM of the inner cyst layer showing also the paracingulum (arrow) and the flattened shape of cysts. Scale bar = 10 μm.

matics platform at http://www.atgc-montpellier.fr/phyml/ for PhyML analyses.

To elucidate in greater detail the relationship between the dinoflagellates of particular interest we compiled a second alignment comprising the boxed-in species in Fig. 75. Since these dinoflagellates had very similar LSU rDNA sequences we were able to include the divergent domain D2. For this phylogenetic inference we used the type species of *Gymnodinium* (viz. *Gym. fuscum*) as outgroup. Posterior probabilities in BA and bootstrap values (100 replications) in ML were performed to obtain an understanding of the robustness of the tree topology (Fig. 76).

We used PAUP* to estimate the divergence between unique sequences (Table 2). Since some of the determined LSU rDNA sequences were identical, only a single representative sequence was included in all pair-wise comparisons (indicated in Table 2). Estimates of pair-wise comparisons were based on the Kimura two-parameter model. The sequence divergence estimates included 963 base pairs.

RESULTS

Levanderina gen. nov.

DESCRIPTION: Unarmoured dinoflagellates with U-shaped apical groove surrounding the cell apex and opening on the ventral side of the cell. Apical groove with three rows of vesicles. Nuclear envelope without vesicular chambers. Nucleus connected to the flagellar apparatus via a finger-like projection. Chloroplasts present. The sulcus divided into an inner tube containing the longitudinal flagellum and an outer, open furrow. Cell division in the motile stage.

TYPE SPECIES: *Levanderina fissa* (Levander) *comb. nov.*

BASIONYM: *Gymnodinium fissum* Levander (1894. *Acta Societas pro fauna et Flora Fennica* 12 (2), pp. 43–50, pl. 2, figs 5–20).

TAXONOMIC SYNONYMS: *Gyrodinium pavillardii* Biecheler 1952, p. 42, figs XIX, LXVII–LXX, *Gyrodinium uncatenum* Hulburt 1957, p. 210, pl. 4, figs 1–3, *Gyrodinium instriatum* Freudenthal & Lee 1963, p. 183, figs 8–17, *Gymnodinium instriatum* (Freudenthal & Lee) Coats in Coats & Park 2002, p. 522, *Gymnodinium uncatenum* (Hulburt) Hallegraeff 2002, p. 40.

ETYMOLOGY: The genus is named after Prof. Kaarlo Mainio Levander (1867–1943), *primus motor* in marine plankton research in Finland. Prof. Levander found and described the type and presently only species of the genus.

All strains studied by us had essentially the same morphology and although some variation was noted, no consistent differences were observed (Figs 1–12). Cells were characteristically ovoid and varied from spherical to slightly laterally or dorsoventrally compressed. All strains exhibited considerable variation in cell size. Dividing cells and planozygotes with two longitudinal flagella were frequent in the cultures. *Levanderina fissa* strain K-1769 from the type locality (Figs 1–4) measured 21.9–49.4 μm in length and

←

Fig. 32. Details of the ornamented cyst surface and the features of paracingulum: two parallel ridges (arrowheads) and concentric circular structures (arrow). Scale bar = 1 μm.

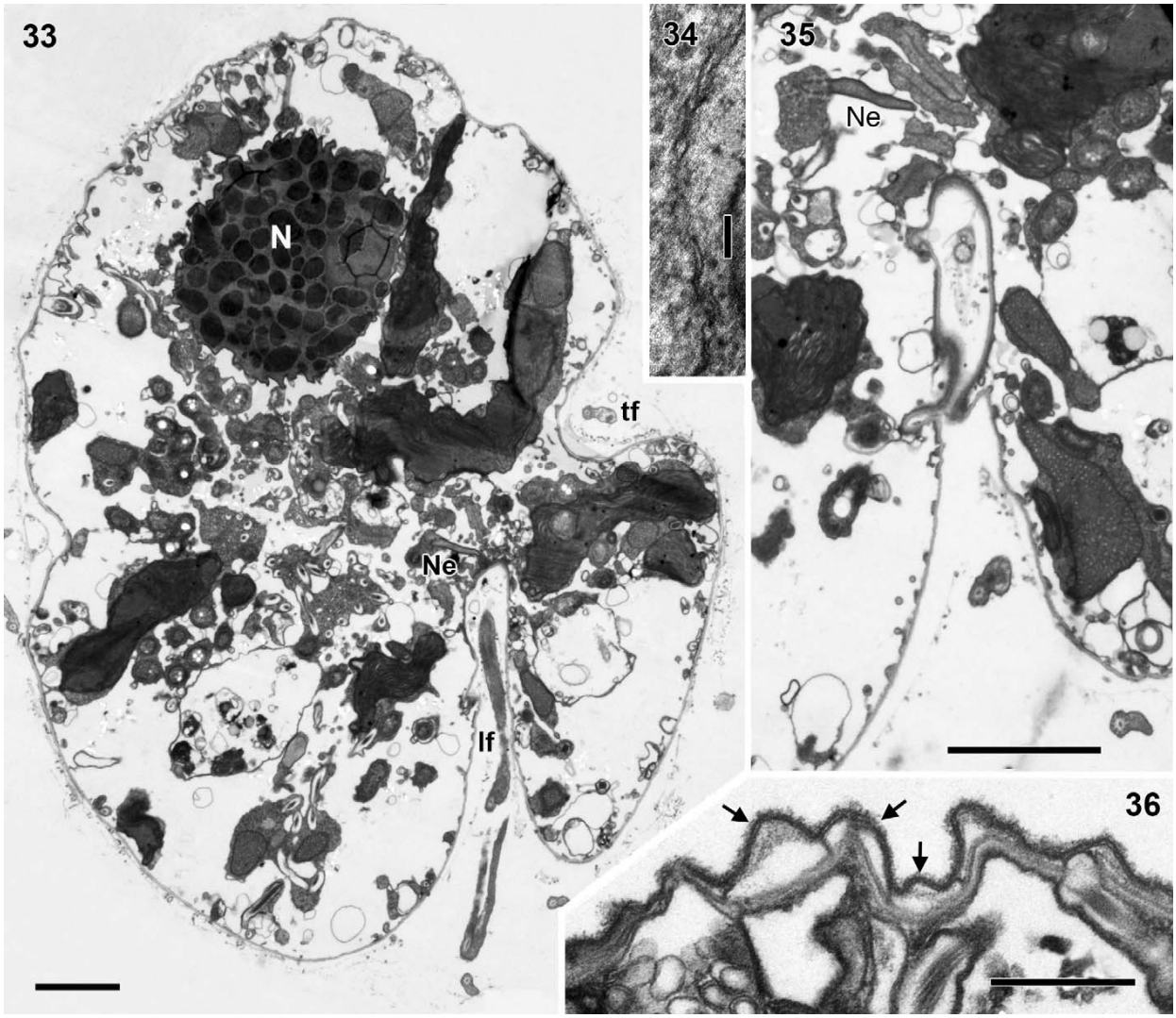

Figs 33–36. *Levanderina fissa comb. nov.*
Fig. 33. Longitudinal section of the cell showing anterior nucleus (N), profiles of chloroplasts, cingulum, and the longitudinal flagellar canal. The transverse flagellum (tf), longitudinal flagellum (lf) and finger-like extension of the nucleus (Ne) are also indicated. Scale bar = 2 μm.
Fig. 34. Nucleus with typical nuclear pores. Scale bar = 100 nm.
Fig. 35. From the same series of sections as Fig. 33, illustrating the sulcus opening through narrow canal into the flagellar canal. Scale bar = 2 μm.
Fig. 36. ASC, formed by three rows of amphiesmal vesicles (arrows), the middle row with pores through which mucilage is extruded (compare with Fig. 24). The row on the right on the figure is located at a deeper level in the epicone and forms the groove. Scale bar = 0.5 μm.

16.5–34.8 μm in width ($n = 50$). The epicone of *L. fissa* was rounded (Figs 1, 4, 9) or truncated (Figs 7, 11), a variation also observed within the strains. The hypocone was bilobed as the sulcus extended to the antapex (e.g. Figs 1, 8, 9). Cingulum was equatorial, spiralling steeply down on the right ventral side, with a cingular displacement of approximately 1/2–1/3 the cell length. The transverse flagellum extended in the cingulum (Figs 7, 12) and the longitudinal flagellum emerged from the excavate hypocone. In the light microscope, the apical groove was discernible in all strains (Figs 1, 3, 5, 7–9, 11, 12), although not in every cell. The U-shaped apical groove encircled the apex and will be described in more detail in SEM (see below). In some specimens deep, longitudinal furrows were observed on the cell (Fig. 10). The large, spherical nucleus was located in the epicone (Fig. 4). Cells were yellow-green or yellow-brown in colour, and epifluorescence microscopy revealed elongate chloroplasts radiating from the centre of the cell (Fig. 6). Orange or red assimilation bodies were present in the cingular area or in the hypocone (Fig. 10), particularly in old cultures.

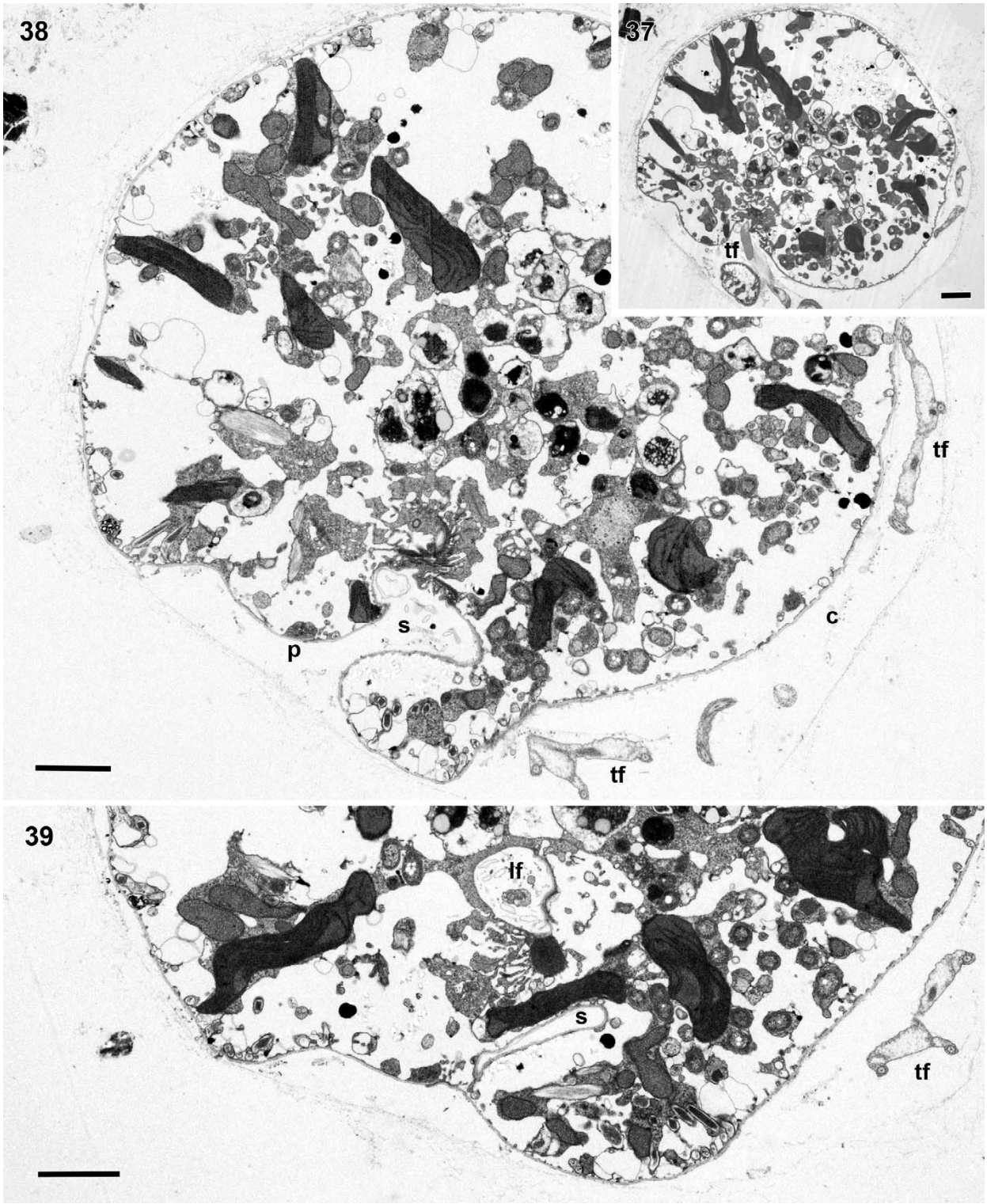

Figs 37–39. *Levanderina fissa comb. nov*. Three sections from a series of transverse sections through the cell at the level of the cingulum. The cell is seen from above, i.e. the cell's left is on the viewer's right. Scale bars = 2 μm.

Fig. 37. Section through the cingulum and the sulcal furrow, showing the transverse flagellum (tf).

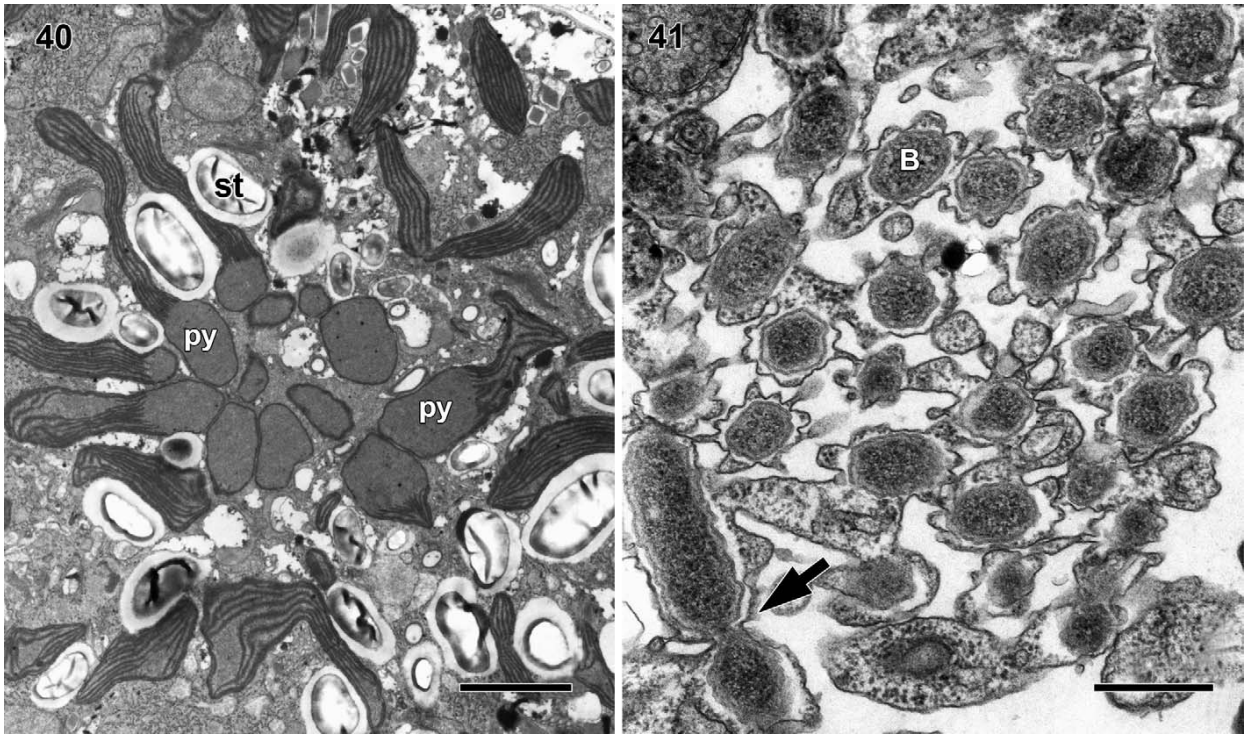

Figs 40, 41. *Levanderina fissa comb. nov.*
Fig. 40. Centrally located complex of pyrenoids (py), a so-called compound pyrenoid, from which extend numerous chloroplasts into the cytoplasm. st, starch grain. Scale bar = 2 μm.
Fig. 41. Clone of *Levanderina* used for fixation and embedding contained numerous bacteria in the cytoplasm, each bacterium (B) enclosed in a vacuole. Some of the bacteria were apparently dividing (arrow). Scale bar = 500 nm.

SEM

SEM revealed the finer details of the cell surface, cingular displacement and apical groove (Figs 13–25). No major differences were observed between the different strains, although strain K-1273 from Puerto Rico had a longer apical groove (see below), and the epicone of this strain generally had more concave sides and a more flat apex. However, the latter features were also observed in cells of the other strains. A few specimens of the strain from Lövö (K-1769) showed faint longitudinal striations (Fig. 15).

The intercingular region, i.e. the right part of the cell between the two ends of the cingulum, was very prominent in all strains. It was triangular in shape, displaced to the left.

A characteristic feature was the deep dorsal incision of the sulcus into the hypocone, and the emergence of the longitudinal flagellum from this dorsal location (Fig. 23).

Many cells formed planozygotes as shown by their duplicated transverse and longitudinal flagella (Figs 15, 19, 21, 25). They were generally considerably larger than the vegetative cells (compare with Fig. 21).

The apical groove and adjacent rows of amphiesmal vesicles, from now on termed the apical structure complex (ASC; for discussion of terminology, see below), was more or less U-shaped and originated from or near a rather indistinct sulcal indentation (Figs 13, 18–20, 22). It continued over the cell apex and about one-third down the dorsal part of the epicone, before terminating 2–3 μm below and to the right of its starting point (Figs 13–25). However, this distance was considerably longer in strain K-1273 from Puerto Rico, usually *c.* 8 μm (Fig. 22), occasionally up to *c.* 12 μm (not shown). The ASC was long, often reaching 30 μm or more from one end of the U to the other. It was composed of three parallel rows of rectangular amphiesmal vesicles. The outermost row comprised rather short vesicles, typically 1.3–1.5 μm long, in which the inner margin was straight, adjoining the second row of vesicles, whereas the outer margin was more irregular, the narrowest parts adjoining the adjacent vesicles.

←
Fig. 38. Section at a slightly lower level showing the sulcal furrow (s) opening to the exterior, with the microtubules of the peduncle (p) located at the right-hand entrance to the sulcal furrow (microtubules not visible at this low magnification; compare with Fig. 46). Parts of the transverse flagellum (tf) are seen in the cingulum (c).
Fig. 39. Section at a somewhat lower level showing the tube containing the longitudinal flagellum (lf). Sulcal furrow (s) appears to be closed to the exterior. tf, transverse flagellum.

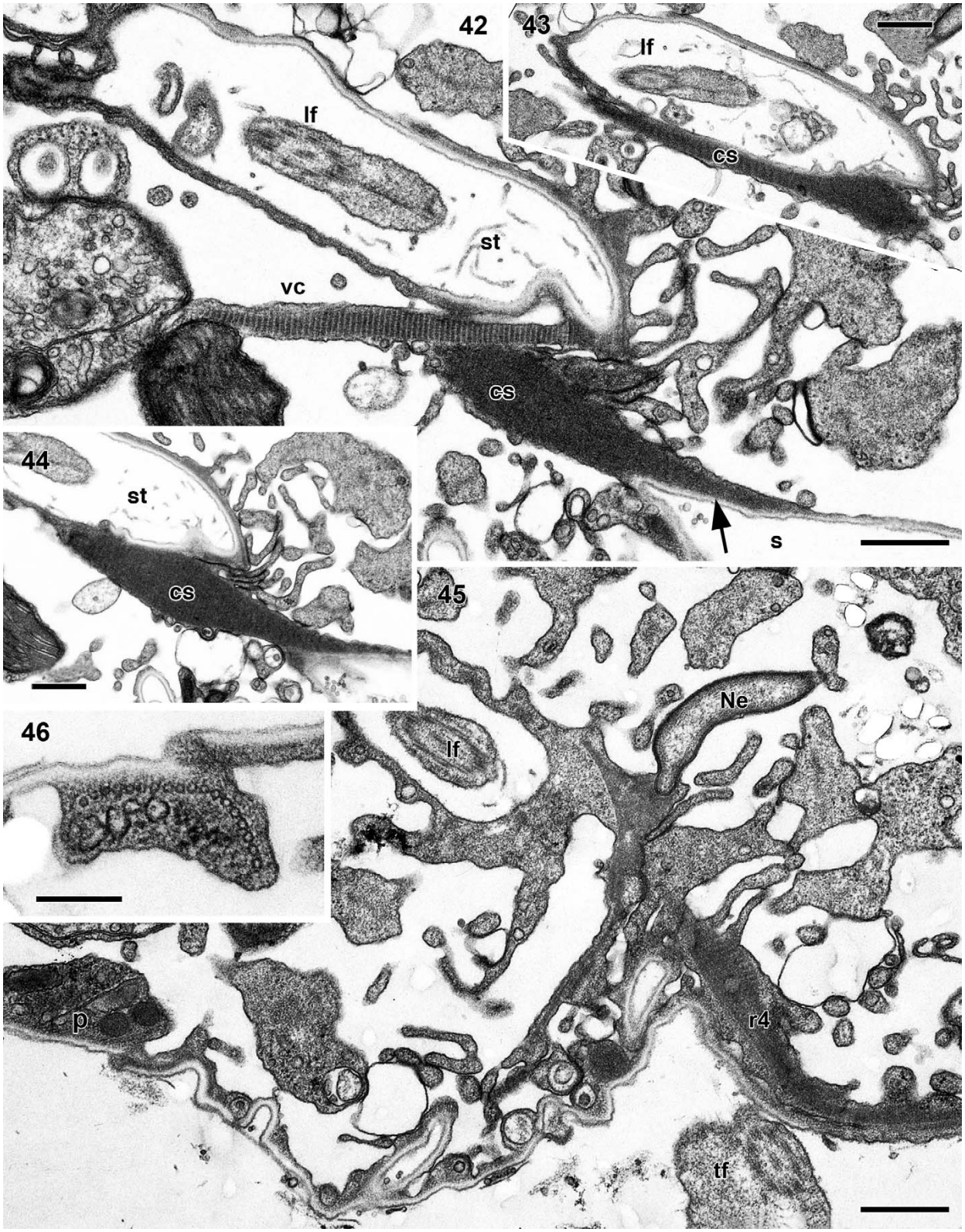
42
lf
st
vc
cs
43
lf
cs
s
44
st
cs
45
Ne
lf
r4
tf
46
p

The middle row was formed by elongate vesicles with parallel sides. The vesicles bore numerous small 'knobs', and delicate fibrillar, probably mucilaginous, material often extruded from the knobs (Figs 16, 24). The length of these vesicles was very variable, from less than 1 to several micrometers, judging from the apparent lack of transverse sutures in the micrographs. The innermost row was more depressed than the other two and comprised the groove *per se* (compare with Fig. 36). Vesicles of this row were elongate with more or less parallel sides, the length very variable from less than 0.5 to *c.* 3 μm, occasionally longer.

The amphiesmal vesicles were not generally visible but covered by membranous material or mucilage. Only in a few cells were they exposed. The vesicles were then observed to be polygonal and measured only about 1 μm across (Fig. 17). The vesicles of the cingulum were more or less quadrangular and arranged in eight rows (Fig. 17).

SEM of strain CCMP 1310 from Falmouth, Massachusetts, USA and available from CCMP as *Gyrodinium uncatenum* proved this isolate to be morphologically identical to *Levanderina fissa* (Bergholtz 2004). SEM of *L. fissa* from Australia was illustrated by Hallegraeff (2002, fig. 10A, as *Gymnodinium uncatenum comb. nov.*).

Resting cysts

Resting cysts were observed both in cultures (particularly older ones) and in the sediment samples from the northern Baltic Sea. Cysts from both sources were morphologically similar. The cysts were circular to ovoid with diameter 54–41 × 48–31 μm (in total 30 cysts were measured from cultures and from the field), and flattened on what appears to be the ventral side (Figs 26, 31), sometimes with indications of paracingulum and parasulcus (Fig. 27). The cyst wall was composed of two layers; the inner layer was colourless and smooth and the outer wall layer a transparent membranous structure, but cysts sometimes lacked this outer layer (Fig. 28). Cyst contents varied from colourless to brownish. The protoplast contained colourless storage granules, lipid or starch droplets, as well as orange-red pigmentation bodies. The nucleus was occasionally visible (Fig. 26). In the SEM samples, most of the cysts were covered by the outer membranous layer (Fig. 29). However, when cysts were found without this layer, the surface of the inner wall was seen to be finely ornamented (Figs 30, 31). Only three cysts were seen without the outer layer. Consistent features in these three specimens were the paracingulum, placed in the middle of the cyst (Fig. 31), and characterized by a fine pattern of two parallel ridges delineating the paracingulum toward the 'hypocone' side and concentric circular structures at uneven distances along the apical side of the paracingular area (Fig. 32). Some cysts had indentations in the surface, but no consistent pattern was noted on the distribution of the indentations, which may be artefacts caused by sample preparation.

TEM

A longitudinal section through the cell is shown in Fig. 33, which illustrates the nucleus, located in the epicone, profiles of chloroplasts, and part of the transverse (cingular) and longitudinal (sulcal) furrows with the flagella. The nucleus extends in a several-micrometers-long, finger-like projection toward the flagellar bases, with which it is connected. It is barely visible at the low magnification in Figs 33 and 35, but shown at higher magnification below (Figs 59–61, 64). The nuclear envelope has typical nuclear pores (Fig. 34), providing direct connection between the nucleoplasm and the cytoplasm. The figures also show the most unusual feature of *Levanderina*, the division of the sulcus into two parallel canals, an inner, longitudinal sulcal tube that is closed at one end and contains the longitudinal flagellum (Fig. 39), and an outer, open longitudinal furrow (s in Fig. 38). The latter is the sulcal furrow visible in the light and scanning electron micrographs, whereas the inner tube is not visible from the outside. The two canals merge at some distance from the antapex (Fig. 35). The apical structure complex is illustrated in transverse section in Fig. 36. The outer row of amphiesmal vesicles is level with the cell surface, whereas the middle row bends over the edge of the apical furrow, part of it forming the side of the furrow. The inner row forms the bottom of the furrow. Adjacent amphiesmal vesicles form the opposite side of the furrow, and curve over the other rim of the furrow.

Transverse sections of the cell provided additional information about cell shape and the furrow system (Figs 37–39). The cingulum did not show unusual morphological features. The longitudinal flagellum in its tube is visible in Fig. 39, several micrometers from the cell surface, whereas the more peripherally located furrow on the ventral side of the cell corresponds to the furrow observed in the SEM. This furrow was usually open to the exterior (Figs 37, 38) but occasionally closed (Fig. 39). A peduncle was not observed in the SEM, but microtubules probably forming part of a peduncle system were always present on the right rim of the sulcal furrow (Fig. 38, in more detail below).

The pusule system was extensive and comprised at least two large canals apparently discharging their contents into the sulcal tube (in detail in Figs 71, 72).

Branches of the chloroplast system were observed almost throughout the cell. Centrally the cell contained numerous aggregated pyrenoids (Fig. 40). They formed a compound pyrenoid system. The pyrenoids lacked penetrating thylakoid lamellae (Fig. 40).

Generally cultures of *Levanderina* grew well, although large numbers of bacteria were often present in the cells,

←

Figs 42–46. *Levanderina fissa comb. nov.* Sections just below the level of the flagellar insertions, showing the tube (st) of the longitudinal flagellum (lf), the sulcal furrow (s), the transverse flagellum (tf in Fig. 45), the very large cross-banded strand (cs), which extends from the cingulum (**Fig. 42**, arrow) to the longitudinal flagellum canal (**Fig. 44**), extending along the latter (**Fig. 43**). **Fig. 42** also shows the vc in its entire length from near the base of the longitudinal flagellum (see further in Figs 56–58) to the surface of a chloroplast/mitochondrion. **Fig. 45** is a general view showing the cingulum with the transverse flagellum, the striated root r4 that extends along the cingulum, the longitudinal flagellum (lf) in the longitudinal flagellum canal, the extension of the nucleus (Ne), and the peduncle (p) on the right-hand side of the cell. **Fig. 46** is a transverse section through the peduncle inside the cell, showing a single row of 18 microtubules. Scale bars = 500 nm (Figs 42–45); scale bar = 200 n (Fig. 46).

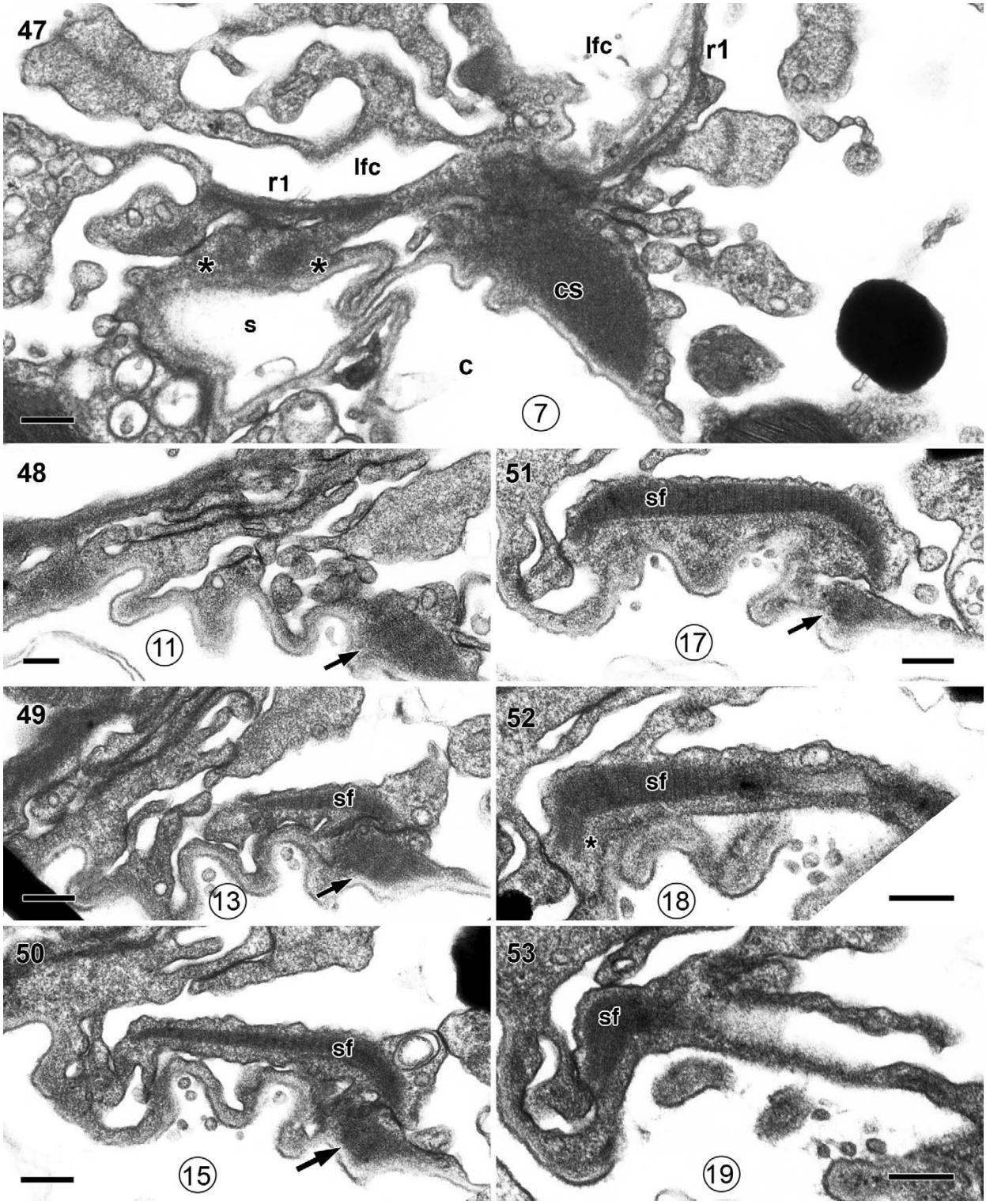

Figs 47–53. *Levanderina fissa comb. nov*. From series of sections at the junction of the transverse and longitudinal furrows. Numbers in circles indicate section number, the direction of sectioning being toward the antapex. The invagination from the exterior labeled s is occasionally seen in this position, and probably represents the longitudinal flagellum furrow, connected to the cingulum (c). The most conspicuous fiber of this region is the cross-banded strand (cs), compare with **Figs 42–44**. It proceeds along the proximal part of the cingulum, gradually becoming

occasionally forming clusters within the cytoplasm (Fig. 41). Each bacterium was located in a vacuole, and dividing bacterial cells were observed, indicating that the bacteria formed a (stable?) symbiosis with its host.

Cytoskeleton

The transversely striated fibre was the most conspicuous component of the flagellar insertion area and extended between the two flagellar canals. It passed along the right-ventral side of the upper part of the sulcal tube (at least 3 μm, Fig. 44), becoming very thick near the bottom of the canal [*c*. 1 μm thick and slightly less wide (Fig. 42, 44)]. The surface of the sulcal tube was irregularly wavy in this region (Fig. 43, also Figs 47 and 54). The strand, which displayed a periodicity of *c*. 80 nm, eventually took up most of (Fig. 42) and eventually the entire area between the proximal part of the sulcal tube and the sulcal furrow (Figs 42, 44). It continued along the proximal part of the sulcal furrow into the cingulum, along the surface of the cingular canal, gradually becoming thinner (Figs 42, 44, 47–51). It passed close to a very distinctly cross-banded muscle-like fibre, which extended along the cingulum/transverse flagellar canal (sf in Figs 49–53), apparently establishing contact with the fibre (Fig. 49). This fibre soon attained a width of *c*. 850 nm and thickness of *c*. 60 nm (Figs 50–52) and was distinctly cross-banded with a periodicity *c*. 37 nm. However, a finer striation could sometimes be discerned between the main bands (barely visible in Fig. 52). The fibre was present in *c*. five consecutive thin sections and must therefore be *c*. 300 nm wide. At the other end it attached to opaque material near the sulcal surface (Fig. 52). The fibre was slightly over 1 μm long, and the surface of the sulcus was often deeply convoluted outside the fibre, indicating that contraction of the fibre had occurred (Figs 49–52).

Peduncle

A structure that we interpreted as a peduncle in a withdrawn state within the cell was always present on the right-hand side of the sulcal furrow (Fig. 45), closely appressed to the cell surface. At higher magnification the peduncle proved to contain a single row of microtubules, located next to vesicles with opaque contents (Fig. 45), and as many as 18 microtubules were counted (Fig. 46), a rather small number for such a relatively large species. The peduncle microtubules extended along the right-hand side of the sulcal furrow but the ends of the peduncle were not identified. We did not observe the peduncle outside the cell, either in the light microscope or in the SEM, but Gaines & Elbrächter (1987, fig. 6.14c) noted a partly emergent peduncle in SEM. On a rare occasion we observed an opaque bulbous structure outside but connected to the peduncle microtubules within the cell (Fig. 73), and this may represent part of the emergent part of a peduncle.

Flagellar apparatus (Fig. 74 diagrammatic illustration)

Two flagella were inserted at an oblique angle of *c*. 145° to one another, the basal bodies being mutually attached by opaque material (Fig. 55). The transverse flagellum was readily identified by its wing-like extension, which started as soon as the flagellum emerged from the cell, extending in the cingulum (Fig. 54). A band of rather stiff hairs was present on the flagellum, but the structure of the hairs and their insertion on the flagellum were not examined in detail. The wing was supported by an opaque rod (perhaps visible in Fig. 38). The longitudinal flagellum, which from its emergence extended into the sulcal tube, carried a short, rather thick wing. This wing was also supported by an opaque rod, and by a thin cross-banded fibre next to the axoneme (Figs 42, 43, also 71 and 72). A tuft of hairs was occasionally seen on the wing, but the hairs were not examined any further.

The flagellar apparatus comprised four microtubular flagellar roots, r1–4, which will be described separately. Root r1 is a band of microtubules that extended from the area above the basal bodies (Figs 59–61), bypassing and attaching to the basal body of the long flagellum (Fig. 63) to continue along the plasmalemma of the sulcal tube (Fig. 55, 67, 71–73). As many as 37 microtubules were observed in this root. Root r1 is a central part of the cell that connected with three major structural components of the cell: (1) On its ventral side a *c*. 0.4-μm-long fibrillar, cross-banded, conical structure (Figs 57, 58) continued into a distinct cross-banded fibre, the ventral connective (vc). The conical structure comprised numerous fibres, which proximally spread out to establish contact with microtubules of the r1 (Figs 57, 58). It comprised two major bands (Fig. 58), a distal and a centrally located band and, in the area between, several less distinct ones. The distal transverse band was attached to the ventral connective, and the latter was *c*. 2.2 μm long and very distinctly cross-banded (periodicity *c*. 30 nm) (Fig. 56). For a short distance the ventral connective passed beneath the sulcal tube (Fig. 42), bypassing the large connecting strand (cs) (Fig. 42, also in Fig. 67), to continue in a straight line on the ventral side of the sulcal tube, and terminating next to a chloroplast and a mitochondrion (Fig. 42). (2) Arising on the opposite side of the r1 was a major, nonstriated rod complex, which extended along the plasmalemma of the sulcal furrow (Figs 54–57). Initially it proceeded as a single rod (Figs. 57, 63), connected to r1 with fine fibers (Fig. 63) but eventually it divided into several parallel opaque rods along or close to the plasmalemma (Figs 59–61, also Fig. 47). In Fig. 73, a cell in which the sulcal furrow was not visible, the group of rods is located midway between the plasmalemma and the sulcal tube (see further in the Discussion).

(3) Arising at some distance from the vc and the nonstriated rod was a large area of opaque material, into which attached a finger-like extension of the nucleus (Figs 59–61, also in Fig.

←
thinner (arrows in **Figs 48–51**). Along the way it bypasses and probably establishes contact with a much shorter but also cross-banded fibre (sf in **Figs 49–52**), which at its other end terminates in opaque material at the cell surface (**Fig. 53**, left). The cavity labeled lfc will eventually develop into the longitudinal flagellum canal, subtended by the microtubules of r1. The sectioning is slightly oblique and also shows the anterior extension of this root (**Fig. 47**). The asterisks in **Fig. 47** indicate opaque rods between the upper part of r1 (compare with Fig. 73) and a short cavity (s) connected to the cingular canal. Scale bars = 200 nm.

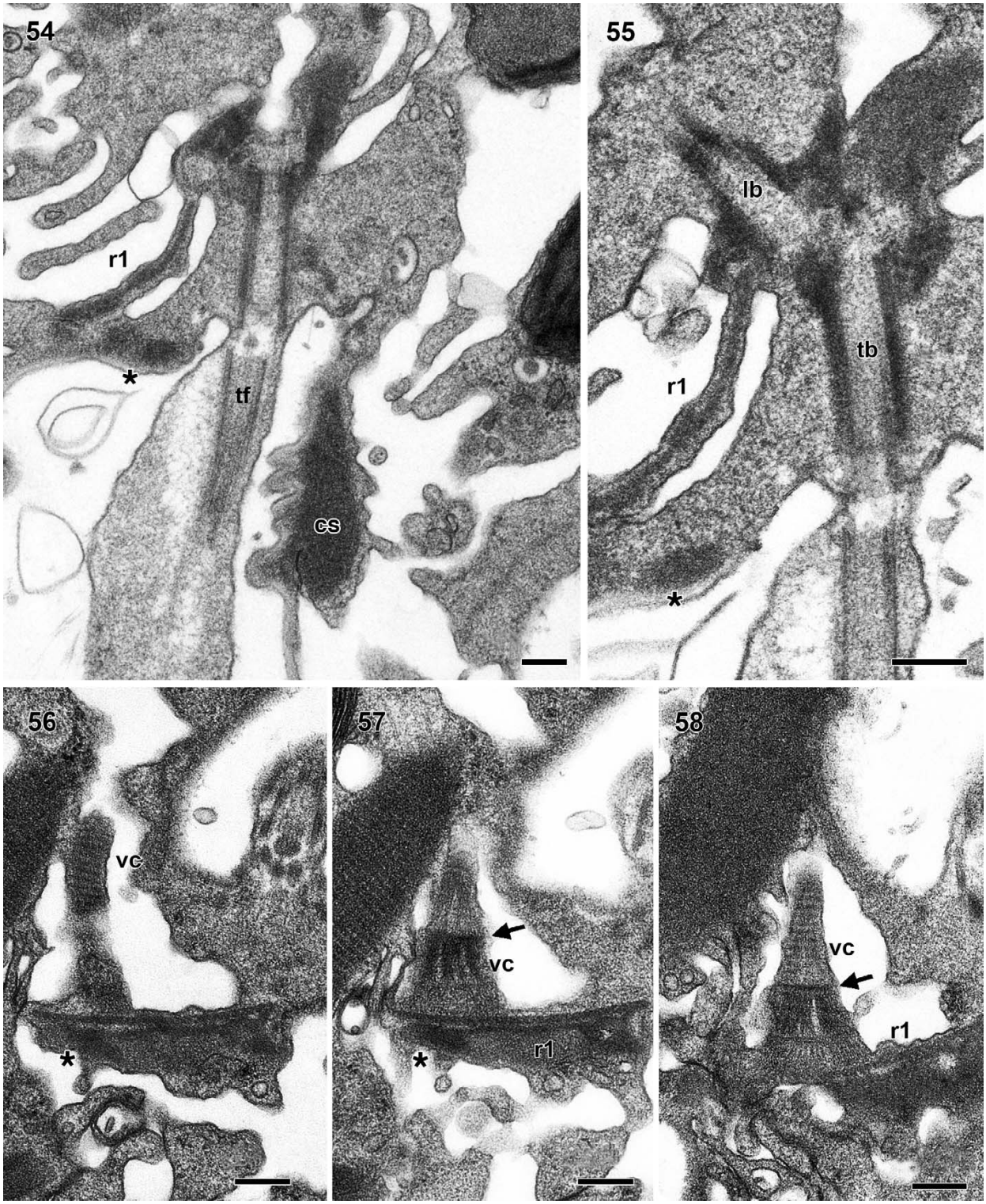

Figs 54–58. *Levanderina fissa comb. nov.* Scale bars = 200 nm.

Figs 54, 55. The two basal bodies (lb and tb) insert at an oblique angle to each other. Root r1 emerges above the level of the longitudinal flagellum base (Fig. 54, compare with Fig. 47) and attaches to the side of the longitudinal flagellum basal body (Fig. 55) before continuing to the posterior part of the cell. The opaque material in Fig. 54 (cs) is part of the large cross-banded fibre (cf. Fig. 42–44), the asterisks indicate the opaque fibres or rods between root r1 and the cingular canal. Tf, transverse flagellum.

45). Considering that the nucleus was located anteriorly in the cell (Fig. 33), the nuclear finger must be relatively long. The finger is visible at its emergence from the nucleus in Fig. 64, for a distance of *c.* 2.5 μm. Its presence in Figs 33 and 35 indicates a length of at least 7 μm. Nuclear pores are visible distally on the nuclear finger in Fig. 64. In a transverse section of the cell, the nuclear finger and the vc were visible on opposite sides of the sulcal tube (Fig. 67). This figure also illustrates that the sulcal tube at its proximal end divides into two shallow extensions. The r1 root initially passed along the ventral extension of the sulcal tube, which was longer than the other, whereas the longitudinal flagellum emerged from the dorsal-most tube (Fig. 67).

The r1 root also included a dorsal striated part, which is readily confused with the r4 root. It is seen best in Figs 69 and 70 and had a periodicity of *c.* 40 μm. The nuclear finger attached indirectly to r1 via the dorsal striated fibre or other fibrous material (nfc in Fig. 74), close to where the flagellar canal divided into the two extensions (Fig. 67).

The root r2 was very short and we have only seen it a few times (Fig. 68 and inset). Only a single, very short microtubule was observed.

The root r3 was present but difficult to study, apparently having a somewhat irregular path. Our micrographs indicate that it began as a single microtubule on the right/apical side of the basal body of the transverse flagellum (Fig. 69). From here it extended to the cingulum, and profiles of the microtubule were seen in several places along the cingulum (Figs 68, 69). Along the microtubule were seen at least four groups of (usually) triplets of microtubules (Figs 68, also 66), apparently nucleated by r3.

The root r4 was rather short, and started proximally in a rather compact mass of opaque material on the left-hand side of the basal body of the transverse flagellum, almost opposite the emergence site of Fig. 68. A striated component with a periodicity of 30–35 nm soon became visible, as shown at higher magnification in Fig. 65. The root proceeded from the basal body to the canal of the transverse flagellum (Fig. 45), and then extended along the cingulum for some distance. A fan-shaped conical connecting fiber (TB/r4c) was present between the root and the basal body of the transverse flagellum (Fig. 70). A structure somewhat reminiscent of the striated root component of many other dinoflagellates was occasionally seen (Fig. 70 and inset). It comprised an opaque central layer, surrounded on each side by a thinner less opaque layer.

Molecular phylogenetics

A phylogenetic analysis based on partial, nuclear-encoded rDNA sequences for a diverse assemblage of dinoflagellates is shown in Fig. 75. The dinoflagellates of the tree comprised a highly supported monophyletic group (posterior probability =1 and bootstrap = 100%). However, the relationship between the deepest lineages was not resolved using this data matrix, which was based on partial, nuclear-encoded LSU rDNA. Yet major groups, which may represent orders, families or genera, were strongly supported (Fig. 75). The dinoflagellate strains studied in the present work formed a clade that obtained maximum support both in terms of posterior probability and bootstrap. The branch length leading to the clade was relatively long, indicating the distinctiveness of the strains. On the basis of molecular data they were as unique as the recently described dinoflagellate genera *Moestrupia* (Hansen & Daugbjerg 2011), *Tovellia* and *Jadwigia* (Lindberg *et al.* 2005), the family Kareniaceae (Bergholtz *et al.* 2006) and even the order Dinophysiales, representing different taxonomic levels. On the basis of these results the novelty of the cultures matched at least the generic level. The branch length leading to the 11 cultures examined here were very short, indicating that their sequences differed very little. This was also supported by the sequence divergence estimates (Table 2). The relationship within this clade was generally not resolved by posterior probabilities or bootstrap values, yet posterior probabilities proposed a subgroup comprising the two strains presently identified as *Gyrodinium instriatum* (K-1067 and K-0675), strain K-1769 and the two isolates from Åland (K-1727 and K-1768).

Reducing the taxon sampling to *Gymnodinium fuscum* and the 11 dinoflagellates of particular interest allowed us to include the divergent domain D2 in the alignment. Using this as input for phylogenetic inference we obtained a second BA tree (Fig. 76). The branch lengths were still short but the two cultures of *Gym. instriatum* and the cultures from Lövö and Åland again formed a highly supported clade also in terms of bootstrap values (96%; posterior probability = 1.0). The other branches received low support, indicating that the proposed tree topology for these lineages was not significant (Fig. 76).

Table 2 reveals similarity estimates between LSU rDNA sequences (including the highly divergent domain D2) for the 11 dinoflagellate cultures indicated by a grey box in Fig. 75. When comparing *Gymnodinium fuscum* with each of the seven unique LSU rDNA sequences the divergence was found to be 23.9–25.3%. The divergence between the seven unique LSU rDNA sequence was 0.13–1.71%. The highest value was between K-1768 and K-1273 and the lowest between K-675 and K-1727/K-1067/K-1769.

DISCUSSION

The cells from the type locality of *Gymnodinium fissum* agreed well with Levander's description. The most contentious issue, the presence of very fine longitudinal lines observed in a few cells by Levander (1894, p. 46), was, as mentioned above, confirmed, but usually cells did not show any striation, either in the light or in the scanning electron microscope. Selected drawings from Levander's work are reproduced here as Fig. 77. Very significantly, Levander did not see or illustrate the longitudinal flagellum inside the longitudinal furrow. He drew cells with an indentation at the

←

Figs 56–58. Serial sections through the point of attachment of the vc to the ventral side of root r1. Ventral connective terminates in a transverse plate (Figs 57, 58, arrow) from which a very complex conical structure connects to r1. The conical structure is composed of fine longitudinal fibres and cross-banded. Asterisks indicate the opaque rods located on the opposite side of r1.

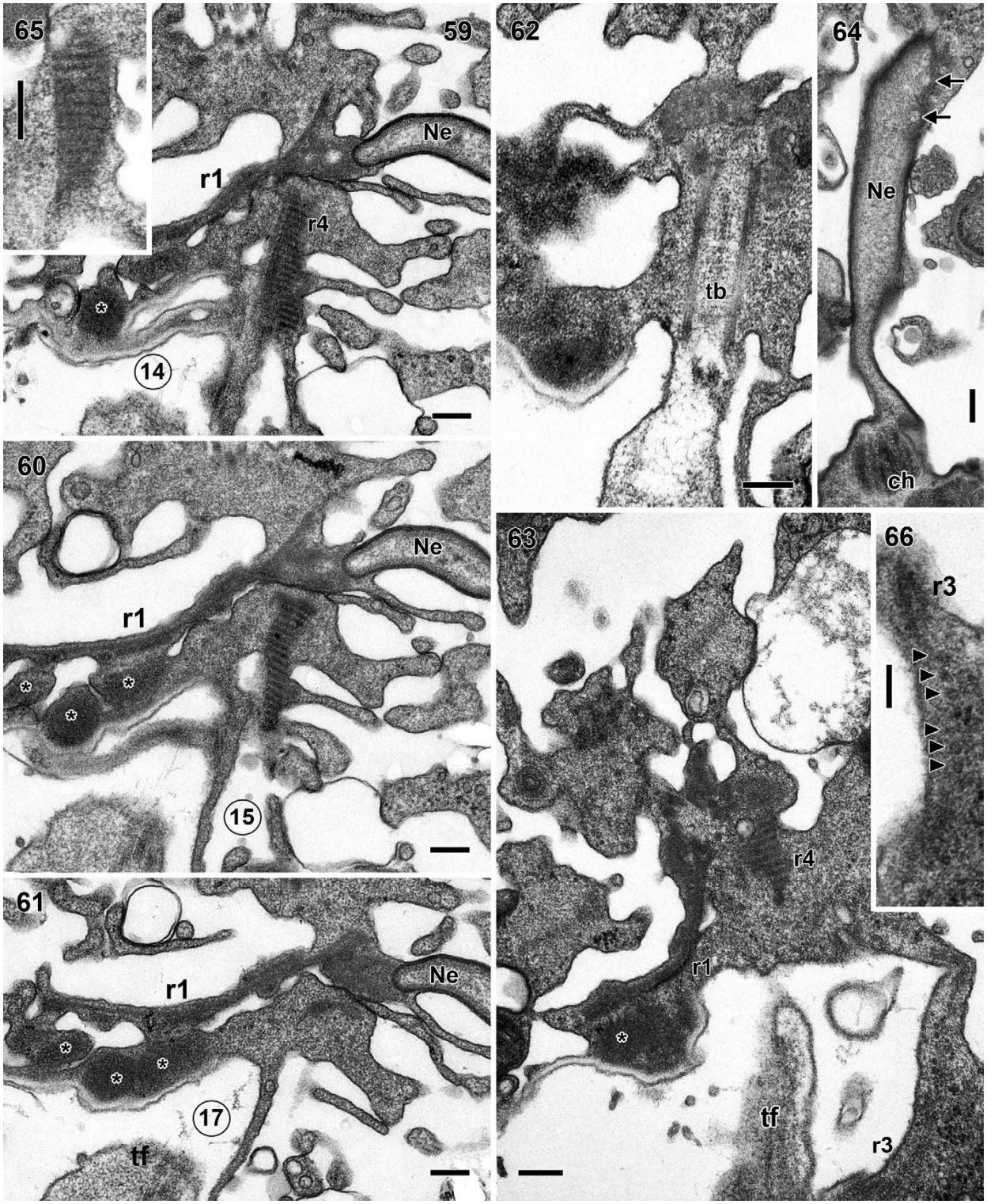

Figs 59–66. *Levanderina fissa comb. nov.*

Figs 59–61. Sections from a series through the proximal part of r4, on the surface of the transverse flagellum basal body. Section numbers in circles. The r1 flagellar root bypasses the basal body and establishes contact with the distal end of the finger-like extension of the nucleus (Ne). Scale bars = 200 nm.

antapical end and visible also from the dorsal side, and the longitudinal flagellum is seen to emerge from this part of the cell, 'also ziemlich weit von dem Ausgangspunkte der Quergeissel' (rather far from the emergence point of the transverse flagellum). This is exactly as observed in the present material and illustrated in Fig. 23. In our Fig. 19 two longitudinal flagella emerge from the sulcal tube, and in fact Levander in his fig. 5 also drew two longitudinal flagella in this position (our Fig. 77a) and commented that cells with two longitudinal flagella were more common than cells with a single flagellum. This we know now indicates that fusion of gametes had taken place in Levander's original material from 1892 to 1894 and was confirmed in our material from the same locality.

Levander's drawings also illustrate cell division, which was followed from the beginning of nuclear division to cytokinesis, the whole process lasting *c.* 1½ h. The longitudinal flagellum was illustrated throughout cell division in one of the daughter cells, but no other flagella were illustrated. This agrees with the theory of flagellar replication in dinoflagellates, which postulates that the longitudinal flagellum remains as such in the next generation, whereas the transverse flagellum transforms into a longitudinal flagellum in the other daughter cell. Both daughter cells develop new transverse flagella (Heimann *et al.* 1995).

Mixotrophy

Our preliminary experiments with feeding failed. We therefore initially suspected that *Levanderina* only fed on very select organisms, a situation that has its parallel in *Dinophysis* (Park *et al.* 2006). There is no doubt, however, that *L. fissa* is mixotrophic. Levander (1894), when describing the species for the first time, included a drawing in which the cell contained a large pennate diatom in the cytoplasm (his fig. 12, reproduced here as Fig. 77G), probably the first demonstration of mixotrophy in dinoflagellates. The diatom is actually longer than the dinoflagellate host, which is somewhat distorted anteriorly. On another occasion Levander found an 'elongate structure, not a diatom', within the cell. Levander worked with mixed samples from nature. Biecheler (1952, p. 124), however, described in detail how *Gyrodinium pavillardii* (which we consider to be identical to *L. fissa*) ingested a small phototrophic dinoflagellate that in her samples co-occurred with *Gyrodinium*. She was unable to see how contact between prey and predator was established but described food uptake to take place at the level of the longitudinal furrow. She subsequently discovered and described in more detail how *Gyrodinium* fed on the ciliate *Strombidium*. When a swimming *Strombidium* happened to hit the apical end of *Gyrodinium*, nothing happened, and the two cells again moved apart. However, if a passing cell of *Strombidinium* hit the antapical end of *Gyrodinium*, *Strombidium* stopped swimming instantaneously, becoming and remaining immotile. Its trichocysts were not discharged. *Strombidium* remained attached to the antapical end of the sulcus, which then widened throughout the entire length of the sulcus to form two lips: a 50-μm *Gyrodinium* was capable of ingesting a *Strombidium* that was 40 μm long and 25 μm wide! Ingestion took some 10 min and *Gyrodinium* remained swimming throughout ingestion and digestion, the latter process taking 5–6 h. Our findings of peduncle microtubules close to the right-hand side of the sulcal furrow supports *Levanderina* as mixotrophic. Another question is, however, how feeding takes place in detail. The evidence so far indicates that the peduncle and the sulcal furrow are involved, and it supports Biecheler's observations that the sulcal furrow plays a central role in food uptake: the sulcal furrow often appeared very irregularly wavy in our sections. The wavy appearance of the proximal part (bottom) of the furrow indicated that it may change shape during feeding, and this is supported by the finding of at least three systems of putative contractile fibres in the area. The SEM showed the bottom of the sulcal furrow to contain a longitudinal ridge (Fig. 19), whereas in some thin sections the sulcal furrow appeared to be absent, the area instead possessing several shallow invaginations. Four such invaginations are visible in Fig. 48. In the scanning micrograph in Fig. 21 the proximal part of the sulcal furrow is very narrow. This may be a response to the treatment for SEM and it proves that this whole area is highly labile. Further experimentation is required to study details of the feeding process, but the involvement of the sulcus as a feeding structure and the relegation of the longitudinal flagellum to a separate internal tube are presently unique. Considering Levander's and Biecheler's observations, *Levanderina* is not choosey when it comes to food, and feeding with diatoms, small dinoflagellates or *Strombidium* should be attempted for further studies on food uptake.

Phylogeny

In the present study all strains within the *Levanderina* clade formed a well-supported clade. The small genetic differences between the different strains suggested that they represent the same species with *L. fissa* as type for the monospecific genus. However, two distinct subgroups within '*Gyrodinium instriatum*', perhaps representing two species, were recently demonstrated on the basis of internal transcribed spacer (ITS) sequences (Stern *et al.* 2012). One group consisted exclusively of strains from China (Shao *et al.* 2004), suggesting a biogeographical separation (Stern *et al.* 2012). A detailed morphological analysis of these strains would be very interesting, for comparison with the data presented in the present study.

It has long been clear from the molecular trees published that the two taxa identified as *Gyrodinium instriatum* and *Gyr.*

←

Figs 62, 63. Two to three opaque fibres pass along the dorsal side of r1 (asterisks) but fuse into a single unit along the canal of the transverse flagellum. Tb, transverse flagellum basal body. Scale bars = 200 nm.

Fig. 64. Finger-like extension of the nucleus (Ne), and nuclear pores in the nuclear envelope are visible at the top of the picture (arrows). Scale bar = 200 nm.

Fig. 65. Transverse striation of the r4 root at higher magnification. Scale bar = 200 nm.

Fig. 66. The r3 root and its extension of microtubules (arrowheads) along the canal of the transverse flagellum. Scale bar = 100 nm.

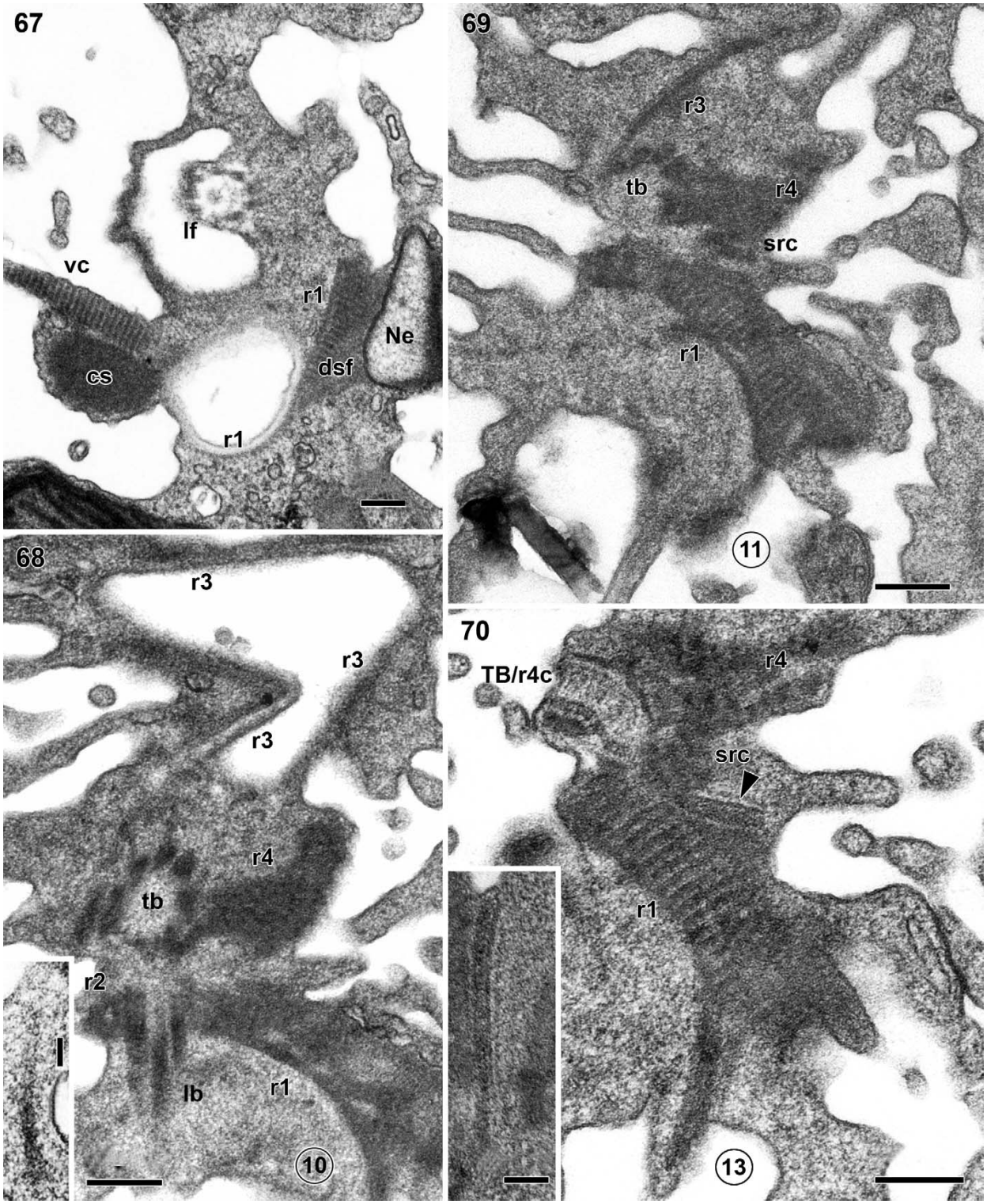

Figs 67–70. *Levanderina fissa comb. nov.*

Fig. 67. The r1 root from its association with the nuclear finger (Ne) extends along the pocket of the longitudinal flagellum canal. The nuclear finger attaches to the dorsal striated part (dsf) of the r1. The vc fibre and the large cs are also visible in this region. Scale bar = 200 nm.

uncatenum are only remotely related to *Gyrodinium*. The two taxa, in the present work renamed *Levanderina fissa*, never cluster with other species of *Gyrodinium*. *Levanderina* sometimes forms a sister group to the Kareniaceae [on the basis of small subunit (SSU) rDNA, Kang *et al*. 2011], or to *Akashiwo sanguinea*, the two then forming a sister group to the Kareniaceae (on the basis of LSU rDNA, Reñé *et al*. 2011). Logares *et al*. (2007) showed the *Levanderina* group as a sister to a clade comprising *Glenodiniopsis steinii*, *Gymnodinium impatiens* and *A. sanguinea* (on the basis of SSU rDNA). *Levanderina* never forms a sister group to true *Gymnodinium*, i.e. the group that includes the type species *Gym. fuscum* (SSU, Saldarriaga *et al*. 2001, and many others). The ultrastructural data also demonstrate considerable difference between *Gymnodinium* and *Levanderina*, *Levanderina* lacking characteristic features of the *Gymnodinium* group such as nuclear chambers and a distinct nuclear fibrous connective. The true phylogenetic position of *Levanderina* is, however, still somewhat ambiguous. If the structure of the ASC proves to being shared between *Gymnodinium* and *Levanderina*, a relationship to the Gymnodiniaceae is likely, although this is not supported by the molecular data. *Levanderina* is presently unique in its use of the sulcus, which in other dinoflagellates always contains the longitudinal flagellum. Most likely, in the ancestor of *Levanderina*, the sulcus was divided up to serve a dual function, the innermost part forming a tube containing the beating longitudinal flagellum. The strain created in this part of the cell by the beating of the flagellum is counterbalanced by the r1 microtubules along the tube. The outer part of the sulcal complex, here called the sulcal furrow, is no longer associated with the longitudinal flagellum but has gained a different function. Judging from its proximity to the point of insertion of the peduncle, it appears likely that it is indeed involved in food uptake as suggested by Biecheler. The morphology of the sulcus is the most exceptional feature of *Levanderina* and presently sets it apart from all other dinoflagellates known.

The compound chloroplast, in which all pyrenoids are concentrated centrally in the cell, was originally thought to be a rare type of chloroplast in dinoflagellates. However, in recent years this type of chloroplast has been detected in an increasing number of species, from *Alexandrium catenella* (Whedon & Kofoid) Balech (Hansen & Moestrup 1998), over *Tovellia sanguinea* Moestrup, G. Hansen, Daugbjerg, Flaim & d'Andrea (Moestrup *et al*. 2006), to *Dinophysis acuminata* Claparède & Lachmann (Garcia-Cuetos *et al*. 2010), representing three different orders of dinoflagellates. The functional significance of this arrangement is not clear. The connection between individual pyrenoids is relatively loose, and chloroplasts may under certain conditions lose contact with one another and disperse in the cell, as also reported in the euglenoid *Eutreptiella eupharyngea* Moestrup & Norris (Walne *et al*. 1986).

A somewhat unusual feature of *Levanderina* is the very long narrow finger-like extension that connects the nucleus to the flagellar apparatus, attaching to the dorsal side of the r1 root. The finger is several micrometers long. This recalls the situation described in *Cochlodinium polykrikoides* Margalef, in which a short rather bulky and irregular extension of the nucleus connects to the dorsal side of r1, i.e. to the same location as in *Levanderina* (Iwataki *et al*. 2010). *Cochlodinium polykrikoides* shares the lack of nuclear chambers with *Levanderina* but is otherwise very different, particularly so in the path of the ASC. Molecular trees such as Fig. 74 also do not indicate a phylogenetic relationship between *Levanderina* and *C. polykrikoides*. In typical members of the Gymnodiniales, represented by *Gymnodinium, Lepidodinium* and *Polykrikos*, a fibre, which in some species is cross-banded [the nuclear connecting fibre (NFC)], connects the nucleus to the r1 root. The nucleus may extend more or less into a cone at the point of attachment between the NFC and the nucleus (*Lepidodinium chlorophorum*; Hansen & Moestrup 2005) or, in *Lep. viride*, a *c*. 1-μm-long cylindrical extension of the nucleus is directed toward the flagellar apparatus, surrounded by the NFC fibre, which then proceeds toward the flagellar apparatus, located another *c*. 3 μm away (Hansen *et al*. 2007, fig. 33). A NFC-like structure was also observed in *Biecheleria baltica* of the order Suessiales (Moestrup *et al*. 2009), whereas in most other dinoflagellates, no direct connection has been found between the nucleus and the flagellar apparatus.

The r1 root of *Levanderina* possesses another feature that has been reported very rarely in dinoflagellates, a dorsal striated fibre (dsf) located on the dorsal side of the root. It is readily confused with the striated part of the r4 root located close by. The dsf is presently known in two species only, one of which is *Oxyrrhis marina* (Roberts 1985), presently considered to be one of the most primitive dinoflagellates (e.g. Moestrup & Daugbjerg 2007). In molecular trees, *Oxyrrhis* consistently branches off at the base of the phylogenetic trees, and cells show several unusual morphological features, including mitosis, which is open as in many other protists and thus unlike the closed mitosis with microtubular canals in typical dinoflagellates. *Oxyrrhis* has a very prominent striated component on the dorsal side of the very large (*c*. 50 microtubules) r1 root (labelled sc-pmr in Roberts 1985, figs 16, 17, 22). A similar structure was found by Hansen (1993) in another, very aberrant species, *Actiniscus pentasterias*, a species characterized by cells possessing an internal silicified skeleton (Hansen 1993). Its phylogenetic relationships remain unknown, but another similarity between this species and *Levanderina* is the presence of a distinct, muscle-like, striated fibre (vf), which from the ventral side of r1 proceeds along the

←

Figs 68–70. From series of sections through the basal bodies and the associated flagellar roots, section number in circles. Both basal bodies have been sectioned in Fig. 68, which also illustrates all four flagellar roots. Root r1 is multimembered and shown best in Figs 69 and 70. On its surface is a cross-banded component (Figs 69, 70). The opaque material on the side of the longitudinal basal body represents the short r2 (Fig. 68), which is seen better in the inset. Root r3 takes an irregular path from the side of the transverse basal body (Fig. 68), passing along the transverse flagellum canal. Root r4 is visible as opaque material. Roots r1 and r4 are attached to one another by means of a layered structure (src), comprising a central opaque band, surrounded on each side but a less opaque band (Fig. 70 and inset). The TB/r4c indicates a banded structure that interconnects the transverse flagellum basal body with r4. Scale bars = 200 nm; inset Fig. 68: scale bar = 50 nm; inset Fig. 70: scale bar = 100 nm.

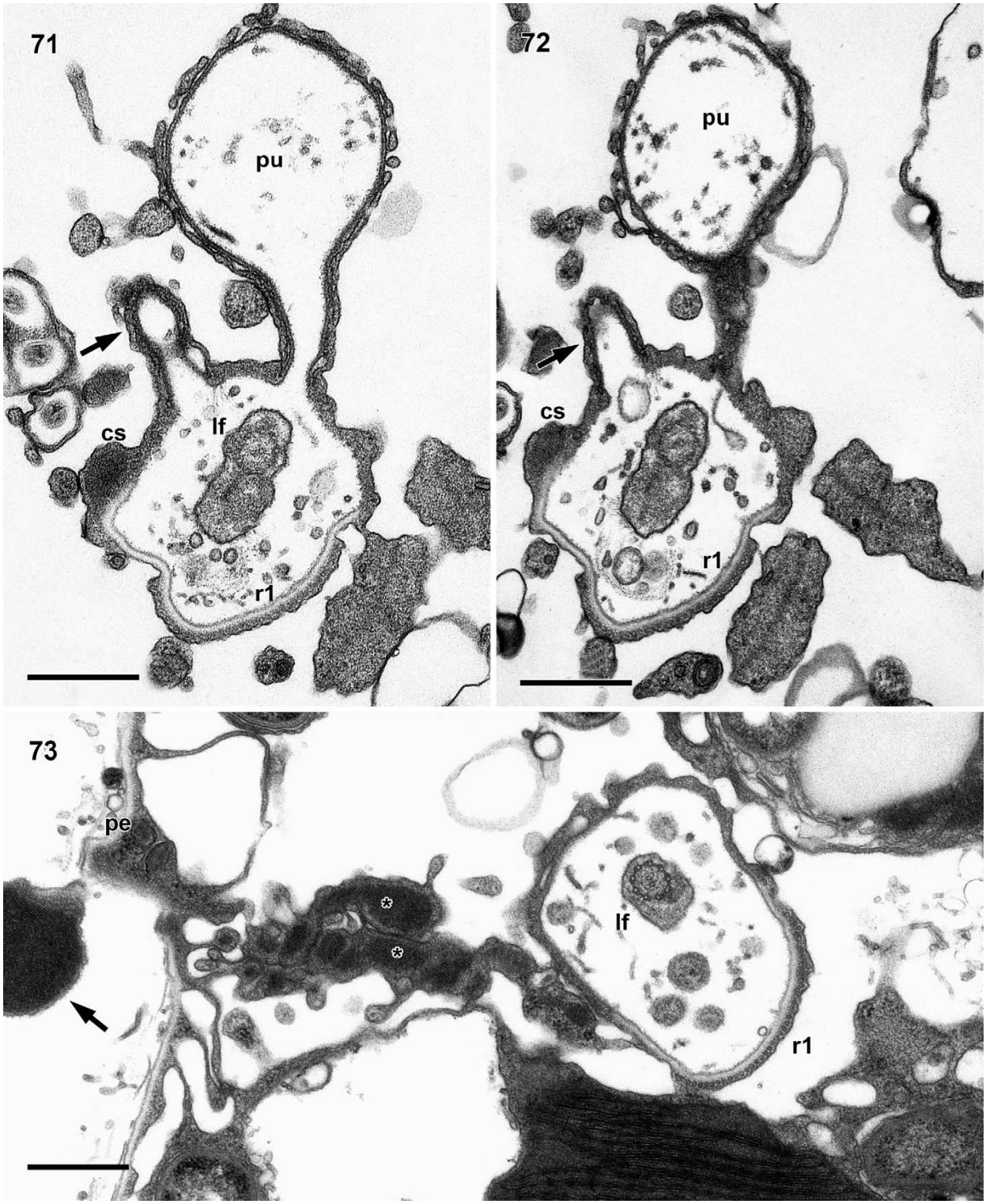

Figs 71–73. *Levanderina fissa comb. nov*. Scale bar = 500 nm.

Figs 71, 72. Transverse sections of the cell at some distance below the insertion of the flagella, showing openings of two pusule canals (pu, and arrow) into the tube of the longitudinal flagellum opposite the insertion of microtubular root r1. The large cs is visible as an opaque structure on the side of the sulcal tube.

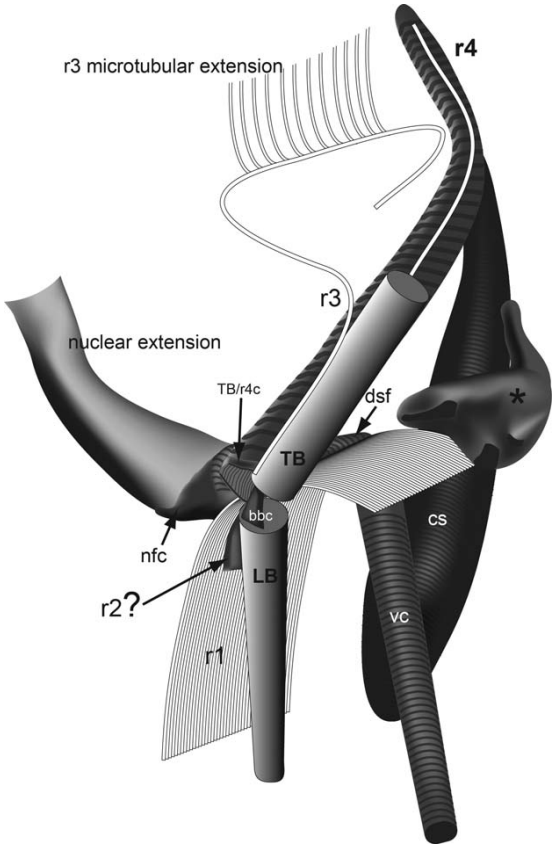

Fig. 74. Diagrammatic representation of the flagellar apparatus of *Levanderina fissa comb. nov.,* as seen in ventral view. Asterisk, the complex of opaque rods between the distal part of r1 and the cingulum; bbc, basal body connective; cs, connecting strand; dsf, dorsal striated fibre; LB, basal body of longitudinal flagellum; nfc, nuclear fibrous connector; r1–4, flagellar roots r1–r4; TB, basal body of transverse flagellum; TB/r4c, connective between root r4 and basal body of transverse flagellum; vc, ventral connective. Striated fibre sf omitted for simplicity.

sulcus. The fibre is attached to r1 by very thin fibres and the whole arrangement is strongly reminiscent of the vc of *Levanderina* and its attachment to the r1. A similar structure, an elongate (at least 5 μm long) muscle-like fibre, extends from the ventral side of r1 in *Akashiwo sanguinea* (Roberts & Roberts 1991) and in *Cochlodinium polykrikoides* (Iwataki *et al.* 2010). In *Levanderina* the vc initially extends toward the sulcal tube, but soon diverges away, to terminate on the surface of a mitochondrion or chloroplast. In *Akashiwo* it apparently extends to the ventral side of the cell (Roberts & Roberts 1991), and in *C. polykrikoides* it runs in an antapical direction, parallel to the longitudinal flagellum canal. A much less prominent structure occurs in this position in certain other species of dinoflagellates such as *Gymnodinium nolleri* (Ellegaard & Moestrup 1999, fig. 34, labeled c2) and *Borghiella dodgei* (Moestrup *et al.* 2008) and connects to the so-called ventral ridge of the cells.

In conclusion, some molecular and some ultrastructural data, in particular the very-well-developed and characteristic vc, indicate a possible phylogenetic relationship between *Levanderina*, *Akashiwo* and *Cochlodinium polykrikoides.* A separate family will most likely need to be erected but it is presently difficult to identify the characteristic features of such as family.

Gyrodinium fissum, GenBank EF613353

The LSU rDNA sequence of *Gyrodinium fissum* from GenBank, accession number EF613353, formed a highly supported sister taxon to a clade comprising *Gyr. spirale* (the type species) and *Gyr. rubrum* (Fig. 75). On the basis of our identifications of *Gyr. fissum* from the type locality we conclude that this material, which originates from coastal waters of Korea, was misidentified. It is a 'true' *Gyrodinium.*

Gyrodinium dorsum UTEX LB 2334

Both SSU and ITS sequences place UTEX LB 2334, deposited as *Gyrodinum dorsum* Kofoid et Swezy, together with *Gyr. instriatum* (Saldarriaga *et al.* 2004; Stern *et al.* 2012). *Gyrodinium dorsum* was originally described by Kofoid and Swezy (1921) from offshore La Jolla, California. It is very different from *Gyr. instriatum*, measuring 72 μm in length, with a posterior nucleus, and although described as having a yellowish colour it seems to lack chloroplasts. We were unsuccessful in obtaining live material of the UTEX strain for closer morphological examination, but on the basis of the pictures of this strain at www.utex.org, there can be little doubt that it represents a misidentified *Levanderina fissa.*

ASC as a phylogenetic indicator

The material of *Levanderina fissa* responded very successfully to the preservation methods used for both SEM and TEM, and this allowed us to obtain information on the detailed construction of the apical furrow apparatus. *Gyrodinium pavillardii*, which appears to be identical to *L. fissa*, was shown by Biecheler (1952, fig. XIX), in silver-impregnated material, to possess a U-shaped 'acrobase', described to be composed of four parallel lines. It undoubtedly represents three parallel rows of narrow amphiesmal vesicles, identical to what we found in *L. fissa.* We introduce the term ASC for the structure variously termed acrobase or apical furrow, as neither of these terms is entirely satisfactory, a furrow is not always present. The path of the ASC on the epicone was used by Daugbjerg *et al.* (2000) to redefine the genera of several gymnodinialean dinoflagellates, and although this has generally worked satisfactorily, it has not contributed toward determining the higher levels of classification: the number of families within the Gymnodiniales, or the definition of the order Gymnodiniales itself. Present molecular evidence indicates that all genera of the '*Gymnodinium* s.s. clade' (Hoppenrath *et al.* 2009; Kang *et al.* 2011) constitute a single family, for which the name Gymnodiniaceae Lankester 1885 is available. The molecular

←

Fig. 73. Area between the cell surface and the sulcal tube in this cell contains a group of opaque rods, some of which are marked with asterisks, but there is no sign of a sulcal furrow. Outside the cell is a large opaque structure, perhaps part of the peduncle (arrow in Fig. 73).

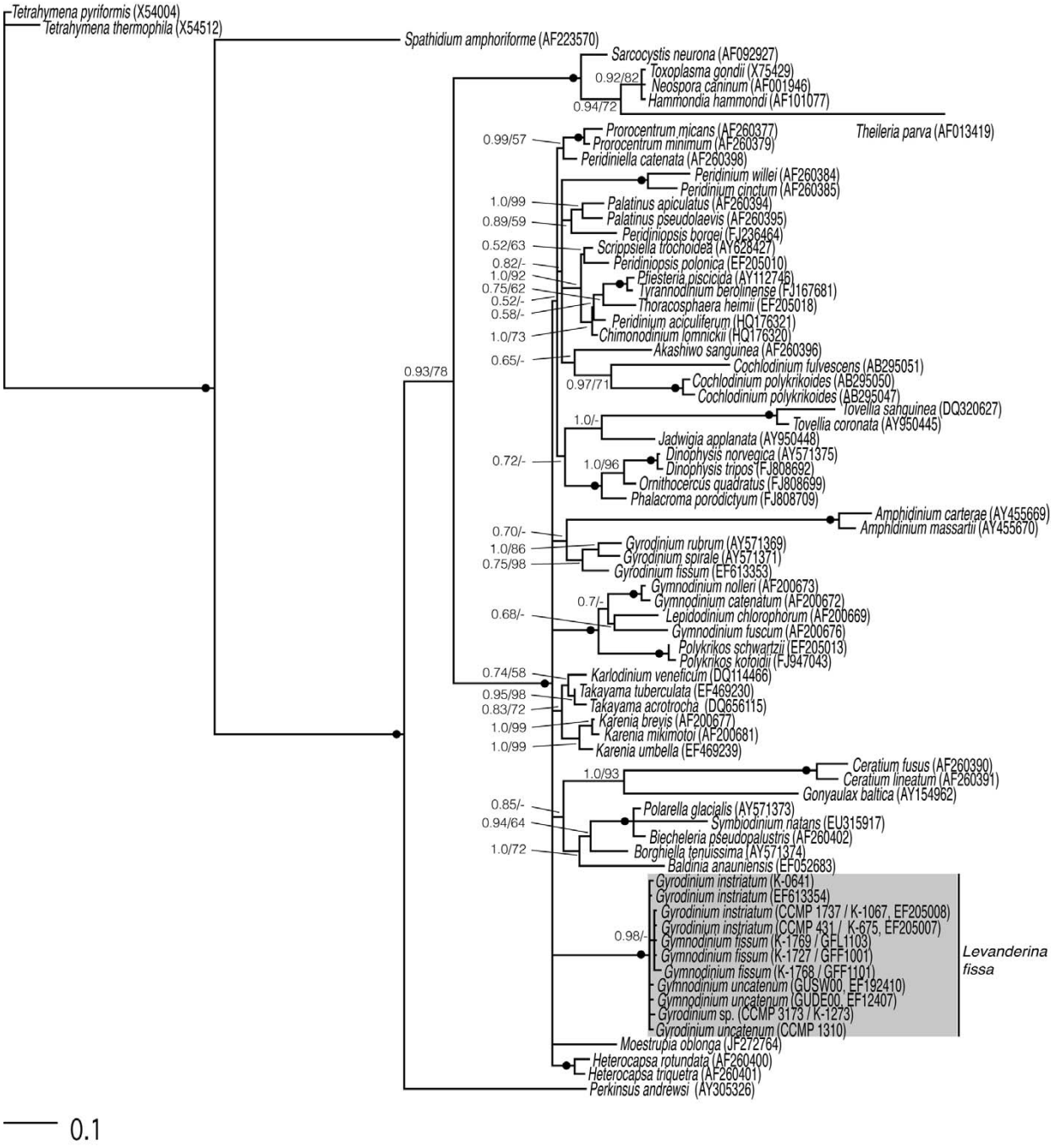

Fig. 75. Bayesian phylogeny of a diverse selection of dinoflagellates (62 species) on the basis of partial, nuclear-encoded LSU rDNA (746 base pairs). Ciliates, apicomplexans and *Perkinsus* form the outgroup taxa. The dinoflagellate cultures of particular interest to this study are boxed in (11 in total). The new genus *Levanderina* proposed in this work replaces the names of all the strains indicated by the vertical line. Posterior probabilities from BA and bootstrap values from ML analyses (100 replications) are noted to the left of internodes. Bootstrap values below 50% are indicated by a '-'. Filled circles indicate maximum posterior probabilities (1.0) and bootstrap values (100%). Strain and GenBank accession numbers are written in brackets.

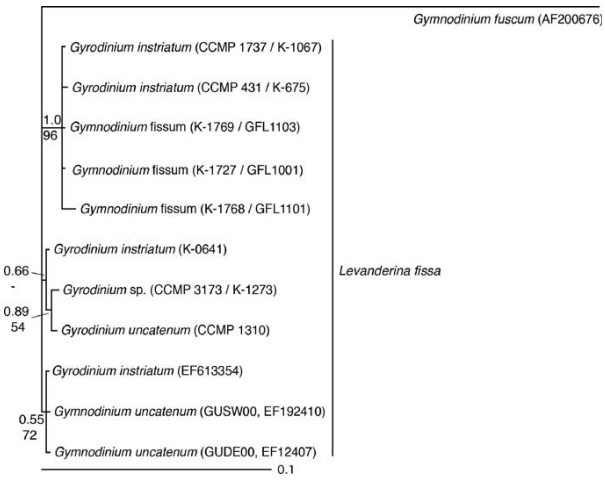

Fig. 76. Bayesian phylogeny of 11 dinoflagellate cultures identified as *Gyrodinium instriatum*, *Gyrodinium uncatenum, Gymnodinium uncatenum* or *Gymnodinium fissum*. *Gymnodinium fuscum* was included to polarize the ingroup. Posterior probabilities from BA and bootstrap values from ML analyses (100 replications) are noted at internodes. Bootstrap values below 50% are indicated by a '-'. Solid circles indicate maximum posterior probabilities and bootstrap values (i.e. 1.0 and 100%, respectively). The alignment included 962 base pairs.

evidence indicates that this may also include the genera usually included in the Warnowiaceae Lindemann 1928 (Hoppenrath *et al.* 2009), although we prefer, for the time being, to retain this as a separate family within the Gymnodiniales. The molecular data do not support inclusion of *Levanderina* in the Gymnodiniaceae, and this, together with the very unusual path of the longitudinal flagellum in a tube, justifies the creation of a new family. The structure of the ASC indicates phylogenetic relationship to other members of the Gymnodiniales, and although there is insufficient and sometimes contradictory information on the structure of the ASC in species of the Gymnodiniales, recent studies indicate similarities. Before going into detail, we notice that in the Suessiales the ASC has been examined in several species, and considerable diversity has been found (presently four types), all of which are different from what has been reported in the Gymnodiniales and in the Tovelliaceae. The latter is a family of somewhat uncertain phylogenetic affinity, in which the species possess an ASC comprising a single row of elongate vesicles (Moestrup *et al.* 2009). Is there a uniform type of ASC in the Gymnodiniales? Sampedro *et al.* (2011), in *Barrufeta bravensis*, a marine gymnodinioid, reported the presence of an ASC comprising three elongated vesicles, the middle row with a line of knobs. The low-magnification micrographs included do not allow further conclusions, but a series of unpublished micrographs sent to ØM for further scrutiny showed three rows of vesicles, sometimes with indication of a fourth row, each row almost certainly comprising several amphiesmal

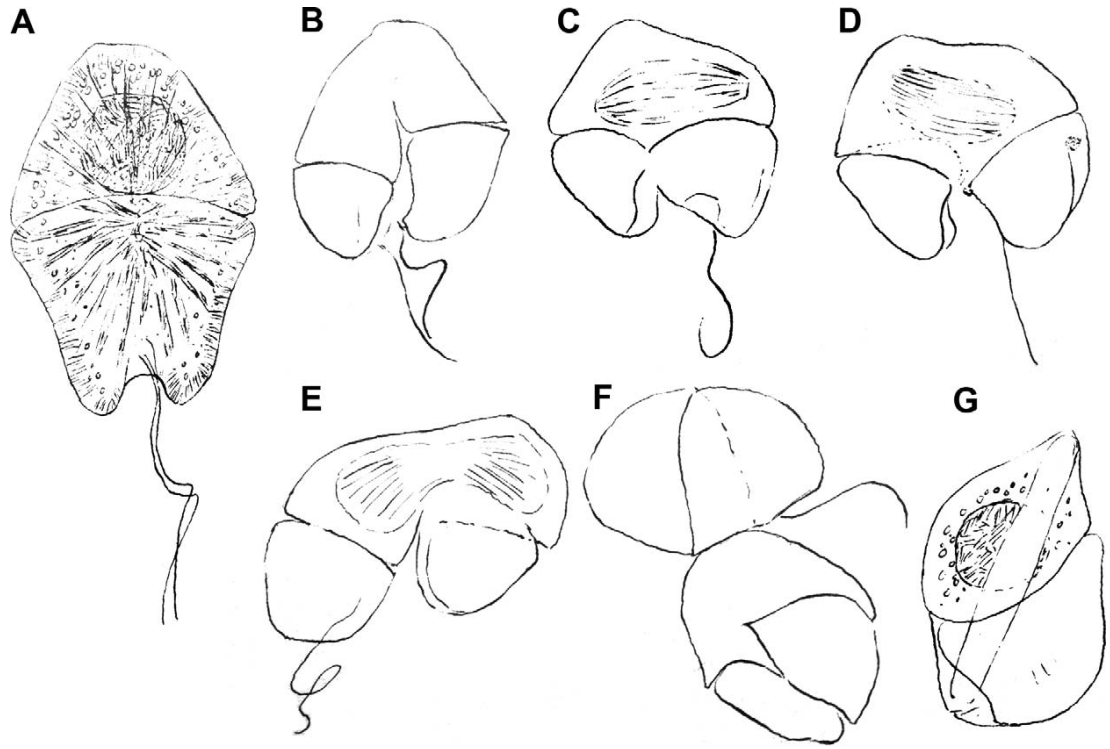

Fig. 77. Selected original drawings of *Gymnodinium fissum* from Levander (1894). (A) A planozygote seen from the dorsal side, the flagella leaving the cell through an invagination on the antapical–dorsal side; (B–F) dividing cells; the cells are dividing in the motile stage; (G) a cell containing an ingested diatom, which is longer than the dinoflagellate, causing some distortion of the cell.

vesicles. The outermost row was a furrow, and although thin sections of the apical apparatus were not included, the evidence indicates an apical apparatus identical to that of *Levanderina*. In *Cochlodinium polykrikoides* the ASC also comprises three rows of vesicles (G. Hansen, unpublished observations). Kang *et al*. (2011) illustrated a 'central ridge' of five elongate amphiesmal vesicles on the epicone of *Gyrodiniellum shiwaense*, another gymnodinioid, and the presence of a row of small knobs on each vesicle, extruding mucilaginous material, indicates it to be homologous to the central row of amphiesmal vesicles in the ASC of *Levanderina*. Whether *Gyrodiniellum* also possesses two additional rows as in *Levanderina* will require additional SEM combined with thin sections, but Kang *et al*. (2011) mentioned that the central ridge was surrounded on each side by an indistinct groove. U-shaped apical grooves were illustrated very recently in '*Proterythropsis*' and *Gymnodinium litoralis* (Hoppenrath *et al*. 2009; Reñé *et al*. 2011), and in the latter species the presence of three elongate vesicles was reported. There is a clear similarity to *Levanderina* in this respect, but additional studies are required to determine whether the three single vesicles reported in *Gym. litoralis* actually comprise three rows of amphiesmal vesicles. Biecheler (1952), using stained cells and light microscopy, drew a single vesicle with knobs in *Gyrodinium vorax*. It was lined on each side by a row of narrow elongate vesicles. This species may belong to the newly described genus *Gyrodiniellum* and, if this can be confirmed, more likely possesses a row of amphiesmal vesicles. On the basis of these studies we hypothesize the existence of a common type of three-rowed apical apparatus (ASC) in many gymnodinioids, including *Levanderina*. Whether it characterizes the entire order Gymnodiniales must await additional data.

Cyst morphology

Recent work has shown that the morphology of the resting cyst (hypnocyst) can be important for distinguishing between genera (e.g. Lindberg *et al*. 2005; Moestrup *et al*. 2009). Descriptions of the cyst of *Gyrodinium instriatum* (Matsuoka 1985; Orlova *et al*. 2003) agree with *L. fissa* in the slightly variable circular to ovoid shape, the transparent, unstructured cyst wall, the cyst content and the surrounding thick mucus layer. Light microscopy images and cyst size of Russian material by Orlova *et al*. (2003, figs 1a, b) also appear identical to our observations on Finnish cells of *L. fissa* (Figs 26–32), whereas they are somewhat wider than Japanese cysts measured by Matsuoka (1985). Light microscopy images of *Gyr. uncatenum* cysts (Tyler *et al*. 1982, figs 9D, E; Coats *et al*. 1984, fig. 21) look indistinguishable from our cysts, which also agree in size (48 × 39 μm: Coats *et al*. 1984). The data available thus support the idea that the many taxa belong to the same species.

The pattern of the inner cyst wall observed in the present study does not correspond to any previously reported cyst type. Cysts of true *Gyrodinium* (*sensu* Daugbjerg *et al*.) are apparently not known. However, the type species of *Gymnodinium*, *Gym. fuscum*, has a very different type of cyst (e.g. Hansen & Moestrup 2000). As presently understood, the morphology of the cyst may represent a unique feature of *Levanderina* and supports it forming a separate genus.

ACKNOWLEDGEMENTS

We thank Guy Hällfors and Anke Kremp for their encouragement when PH isolated the Baltic Sea cultures, Pia Tahvanainen for help in sequencing the Baltic strains, and Charlotte Hansen for technical help running the DNA sequencer. Santiago Fraga kindly provided more information on *Barrufeta*. ND thanks the Villum Kann Rasmussen Foundation and the former Botanical Institute for equipment grants. GH and ØM acknowledge the financial support from the Walter and Andrée Nottbeck Foundation, which covered the expenses of a short stay at Tvärminne Zoological Station in southern Finland during the summer of 2011. PH thanks the Tor Nessling Foundation and the Finnish Cultural Foundation for funding.

REFERENCES

Bergholtz T. 2004. *Undersøgelse af slægten* Karlodinium *(Dinophyceae) baseret på lys- og elektronmikroskopi, LSU rDNA sekvens- og pigmentanalyse*. MSc Thesis. University of Copenhagen. 100 pp.

Bergholtz T., Daugbjerg N., Moestrup Ø. & Fernández-Tejedor M. 2006. On the identity of *Karlodinium veneficum* and description of *Karlodinium armiger* sp. nov. (Dinophyceae), based on light- and electron microscopy, nuclear-encoded LSU rDNA and pigment composition. *Journal of Phycology* 42: 170–193.

Biecheler B. 1934. Sur le réseau argentophile et la morphologie de quelques Péridiniens nus. *Compte Rendus de la Societé de Biologie* 115: 1036–1042.

Biecheler B. 1952. Recherches sur les Péridiniens. *Bulletin Biologique de France et de Belgique* 36, supplement: 1–149.

Coats D.W. & Park M.G.B. 2002. Parasitism of photosynthetic dinoflagellates by three strains of *Amoebophrya* (Dinophyta): parasite survival, infectivity, generation time, and host specificity. *Journal of Phycology* 38: 520–528.

Coats D.W., Tyler M.A. & Anderson D.M. 1984. Sexual processes in the life cycle of *Gyrodinium uncatenum* (Dinophyceae): a morphogenetic overview. *Journal of Phycology* 20: 351–361.

Daugbjerg N., Moestrup Ø. & Arctander P. 1994. Phylogeny of the genus *Pyramimonas* (Prasinophyceae) inferred from the *rbc*L gene. *Journal of Phycology* 30: 991–999.

Daugbjerg N., Hansen G., Larsen J. & Moestrup Ø. 2000. Phylogeny of some of the major genera of dinoflagellates based on ultrastructure and partial LSU rDNA sequence data, including the erection of three new genera of unarmoured dinoflagellates. *Phycologia* 39: 302–317.

Ellegaard M. & Moestrup Ø. 1999. Fine structure of the flagellar apparatus and morphological details of *Gymnodinium nolleri* sp. nov. (Dinophyceae), an unarmored flagellate producing a micro-reticulate cyst. *Phycologia* 38: 289–300.

Freudenthal H.D. & Lee J.J. 1963. *Glenodinium halli* n. sp. and *Gyrodinium instriatum* n. sp., dinoflagellates from New York waters. *Journal of Protozoology* 10: 182–-189.

Gaines G. & Elbrächter M. 1987. Heterotrophic nutrition. In: *The biology of dinoflagellates* (Ed. by F.J.R. Taylor), Botanical Monographs, vol. 21, pp. 224–268. Blackwell Scientific Publications, Oxford, UK.

Garcia-Cuestos L., Moestrup Ø., Hansen P.J. & Daugbjerg N. 2010. The toxic dinoflagellate *Dinophysis acuminata* harbors permanent chloroplasts of cryptomonad origin, not kleptochloroplasts. *Harmful Algae* 9: 25–38.

Gouy M., Guindon S. & Gascuel O. 2010. SeaView version 4: a multiplatform graphical user interface for sequence alignment and phylogenetic tree building. *Molecular Biology and Evolution* 27: 221–224.

Guindon S. & Gascuel O. 2003. A simple, fast, and accurate algorithm to estimate large phylogenies by maximum likelihood. *Systematic Biology* 52: 696–704.

Hallegraeff G.M. 2002. *Aquaculturists' guide to harmful Australian microalgae,* ed. 2. School of Plant Science, University of Tasmania, Hobart. 136 pp.

Hansen G. 1993. Light and electron microscopical obervations of the dinoflagellate *Actiniscus pentasterias* (Dinophyceae). *Journal of Phycology* 29: 486–499.

Hansen G. & Daugbjerg N. 2011. *Moestrupia oblonga* gen. & comb. nov. (syn.: *Gyrodinium oblongum*), a new marine dinoflagellate genus characterized by light and electron microscopy, photosynthetic pigments and LSU rDNA sequence. *Phycologia* 50: 583–599.

Hansen G. & Moestrup Ø. 1998. Fine-structural characterization of *Alexandrium catenella* (Dinophyceae) with special emphasis on the flagellar apparatus. *European Journal of Phycology* 33: 281–291.

Hansen G. & Moestrup Ø. 2000. Light and electron microscopical observations on the type species of *Gymnodinium*, *G. fuscum* (Dinophyceae). *Phycologia* 39: 365–376.

Hansen G. & Moestrup Ø. 2005. Flagellar apparatus and nuclear chambers of the green dinoflagellate *Gymnodinium chlorophorum*. *Phycological Research* 53: 169–181.

Hansen G., Botes L. & De Salas M. 2007. Ultrastructure and large subunit rDNA sequences of *Lepidodinium viride* reveal a close relationship to *Lepidodinium chlorophorum* comb. nov. (= *Gymnodinium chlorophorum*). *Phycological Research* 55: 25–41.

Hällfors G. 2004. *Checklist of Baltic Sea phytoplankton species. Baltic Sea Environment Proceedings No. 95*. Helsinki Commission.

Heimann K., Roberts K. & Wetherbee R. 1995. Flagellar apparatus transformation and development in *Prorocentrum micans* and *P. minimum*. *Phycologia* 34: 323–335.

Hoppenrath M., Bachvaroff T.S., Handy S.M., Delwiche C.F. & Leander B.S. 2009. Molecular phylogeny of ocelloid-bearing dinoflagellates (Warnowiaceae) as inferred from SSU and LSU rDNA sequences. *BMC Evolution and Biology* 9: 116 doi:10.1186/1471-2148-9-116.

Hulburt E.M. 1957. The taxonomy of unarmored Dinophyceae of shallow embayments on Cape Cod, Massachusetts. *Biological Bulletin* 112: 196–219.

Iwatake M., Hansen G., Moestrup, Ø. & Daugbjerg N. 2010. Ultrastructure of the harmful unarmored dinoflagellate *Cochlodinium polykrikoides* (Dinophyceae) with reference to the apical groove and flagellar apparatus. *Journal of Eukaryotic Microbiology* 57: 308–321.

Kang N.S., Jeong H.J., Moestrup Ø. & Park T.G. 2011. *Gyrodiniellum shiwhaense n. gen., n. sp.,* a new planktonic heterotrophic dinoflagellate from the coastal waters of western Korea: morphology and ribosomal DNA gene sequence. *Journal of Eukaryotic Microbiology* 58: 284–309.

Kim K.Y. & Kim C.H. 2007. Phylogenetic relationships among diverse dinoflagellate species occurring in coastal waters off Korea inferred from large subunit ribosomal DNA sequence data. *Algae* 22: 57–67.

Kofoid C.A. & Swezy O. 1921. The free-living unarmoured dinoflagellates. *Memoirs of the University of California* 5: 1–564.

Lemmermann E. 1900. Beiträge zur Kenntniss der Planktonalgen. VIII. Peridiniales aquae dulcis et submarinae. *Hedwigia* 39: 115–121.

Lenaers G., Maroteaux L., Michot B. & Herzog M. 1989. Dinoflagellates in evolution. A molecular phylogenetic analysis of large subunit ribosomal RNA. *Journal of Molecular Evolution* 29: 40–51.

Levander K. M. 1894. Materialien zur Kenntnis der Wasserfauna in der Umgebung Helsingfors, mit besonderer Berücksichtigung der Meeresfauna. I: Protozoa. *Acta Societas pro Fauna et Flora Fennica* 12(2): 3–115, 3 pls.

Lindberg K., Moestrup Ø. & Daugbjerg N. 2005. Studies on woloszynskioid dinoflagellates I: *Woloszynskia coronata* re-examined using light and electron microscopy and partial LSU rDNA sequences, with description of *Tovellia* gen. nov and *Jadwigia* gen. nov. (Tovelliaceae fam. nov.). *Phycologia* 44: 416–440.

Logares R., Shalachian-Tabrizi K., Boltovskoy A. & Rengefors K. 2007. Extensive dinoflagellate phylogenies indicate infrequent marine–freshwater transitions. *Molecular Phylogenetics and Evolution* 45: 887–903.

Matsuoka K. 1985. Archeopyle structure in modern gymnodinialean dinoflagellate cysts. *Review of Palaeobotany and Palynology* 44: 217–231.

Moestrup Ø. & Daugbjerg N. 2007. On dinoflagellate phylogeny and classification. In: *Unravelling the algae: the past, present and future of algal systematics* (Ed. by J. Brodie J. & J. Lewis), Systematics Association Special Volumes, vol. 75, pp. 215–230. CRC Press, Taylor & Francis Group, London.

Moestrup Ø., Hansen G., Daugbjerg N., Flaim G. & D'Andrea M. 2006. Studies on woloszynskioid dinoflagellates II: on *Tovellia sanguinea* sp. nov., the dinoflagellate responsible for the reddening of Lake Tovel, N. Italy. *European Journal of Phycology* 41: 47–65.

Moestrup Ø., Hansen G. & Daugbjerg N. 2008. Studies on woloszynskioid flagellates III: on the ultrastructure and phylogeny of *Borghiella dodgei* gen. et sp. nov., a cold-water species from Lake Tovel, N. Italy, and on *B. tenuissima* comb. nov. (syn. *Woloszynskia tenuissima*). *Phycologia* 47: 54–78.

Moestrup Ø., Lindberg K. & Daugbjerg N. 2009. Studies on woloszynskioid dinoflagellates IV: the genus *Biecheleria* gen. nov. *Phycological Research* 57: 203–220.

Nunn G.B., Theisen B.F., Christensen B. & Arctander P. 1996. Simplicity-correlated size growth of the nuclear 28S ribosomal RNA D3 expansion segment in the crustacean order Isopoda. *Journal of Molecular Evolution* 42: 211–223.

Orlova T.Y., Selina M.S. & Shevchenko O.G. 2003. The morphology of cysts and motile cells of *Gyrodinium instriatum* (Dinophyta), a species new to the seas of Russia. *Russian Journal of Marine Biology* 29: 120–122.

Park M.G., Kim S., Kim H.S., Myung G., Kang Y.G. & Yih W. 2006. First successful culture of the marine dinoflagellate *Dinophysis acuminata*. *Aquatic Microbial Ecology* 45: 101–106.

Posada D. & Crandall K.A. 1998. Modeltest: testing the model of DNA substitution. *Bioinformatics* 14: 817–818.

Reñé A., Satta C.T., Garcés E., Massana R., Zapata M., Anglès S. & Camp J. 2011. *Gymnodinium litoralis* sp. nov. (Dinophyceae), a newly identified bloom-forming dinoflagellate from the NW Mediterranean Sea. *Harmful Algae* 12: 11–25.

Roberts K. R. 1985. The flagellar apparatus of *Oxyrrhis marina* (Pyrrhophyta). *Journal of Phycology* 21: 641–655.

Roberts K.R. & Roberts J.E. 1991. The flagellar apparatus and cytoskeleton of the dinoflagellates. A comparative overview. *Protoplasma* 164: 195–122.

Ronquist F. & Huelsenbeck J.P. 2003. MrBayes 3: Bayesian phylogenetic inference under mixed models. *Bioinformatics* 19: 1572–1574.

Saldarriaga J.F., Taylor F.J.R., Keeling P.J. & Cavalier-Smith T. 2001. Dinoflagellate nuclear SSU rRNA phylogeny suggests multiple plastid losses and replacements. *Journal of Molecular Evolution* 53: 204–213.

Saldarriaga J.F., Taylor F.J.R., Cavalier-Smith T., Menden-Deuer S. & Keeling P.J. 2004. Molecular data and the evolutionary history of dinoflagellates. *European Journal of Protistology* 40: 85–111.

Sampedro N., Fraga S., Penna A., Casabianca S., Zapata M., Grünewald C.F., Riobó P. & Camp J. 2011. *Barrufeta bravensis* gen. nov. sp. nov. (Dinophyceae): a new bloom-forming species from the northwest Mediterranean Sea. *Journal of Phycology* 47: 375–392.

Scholin C.A., Herzog M., Sogin M. & Anderson D.M. 1994. Identification of group- and strain-specific genetic markers for globally distributed *Alexandrium* (Dinophyceae). II. Sequence analysis of a fragment of the LSU rDNA gene. *Journal of Phycology* 30: 999–1011.

Shao P., Chen Y.-Q., Zhou H., Yuan J., Qu L.-H., Zhao D. & Lin Y.-S. 2004. Genetic variability in Gymnodiniaceae ITS regions: implications for species identification and phylogenetic analysis. *Marine Biology* 115: 215–224.

Stern R.F, Andersen R.A., Jameson I., Küpper F.C., Coffroth M.A., Vaulot D., Le Gall F., Véron B., Brand J.J., Skelton H., Kasai F., Lilly E.L & Keeling P.J. 2012. Evaluating the ribosomal internal transcribed spacer. (ITS) as a candidate dinoflagellate barcode marker. PLoS ONE **7**(8): e42780.

Swofford D.L. 2003. *PAUP*: phylogenetic analysis using parsimony (* and other methods), version 4*. Sinauer Associates, Sunderland, Massachusetts.

Tyler M.A., Coats D.W. & Anderson D.M. 1982. Encystment in a dynamic environment: deposition of dinoflagellate cysts by a frontal convergence. *Marine Ecology Progress Series* **7**: 163–178.

Walne P.L., Moestrup Ø., Ettl H. & Norris R.E. 1986. Light and electron microscopical observations on *Eutreptiella eupharyngea* sp.nov. (Euglenophyceae) from Danish and American waters. *Phycologia* 25: 109–126.

Received 19 December 2013; accepted 17 March 2014